

SWART M

OHMIC CONTACTS TO CADMIUM TELLURIDE

MA

UP

1991

Ohmic contacts to cadmium telluride

by

MARTIN SWART

Submitted in fulfilment of part of the requirements for the degree of Masters

in the Faculty of Natural Science

University of Pretoria

Pretoria

May 1991

Ohmic contacts to cadmium telluride

by

MARTIN SWART

Promoter: PROFESSOR F. D. AURET
DEPARTMENT OF PHYSICS
UNIVERSITY OF PRETORIA

Thesis submitted for the degree of M.Sc.

SUMMARY

The problem of manufacturing good ohmic contacts onto cadmium telluride (CdTe) served as a motivation for this study. The accuracy and reliability of the method used to calculate the specific contact resistance of ohmic contacts, will determine the success of any comparison involving different surface preparation and contact manufacturing procedures.

The main objective of this study was therefore to review the different methods most frequently used for determining the specific contact resistance, r_c , and to evaluate their applicability to ohmic contacts on CdTe.

Most of the existing methods are designed for characterizing very good ohmic contacts. The method proposed in this study is recommended to characterize poor to moderate ohmic contacts, which is the case with ohmic contacts on CdTe.

Ohmic contacts to cadmium telluride

deur

MARTIN SWART

Studieleier: **PROFESSOR F. D. AURET**

DEPARTEMENT FISIKA

UNIVERSITEIT VAN PRETORIA

Verhandeling ingedien vir die Meestersgraad

SAMEVATTING

Omdat dit moeilik is om goeie ohmiese kontakte op kadmium telluried (CdTe) te vervaardig, het dit as motivering gedien om elektriese karakterisering van ohmiese kontakte te ondersoek. Om in staat te wees om verskillende oppervlakvoorbereidings en kontakvervaardigings metodes suksesvol te evalueer en vergelyk, is 'n akkurate en betroubare metode om die spesifieke kontakweerstand te bepaal nodig.

Die doel van hierdie studie is dus om die verskillende metodes in gebruik om die spesifieke kontakweerstand, r_c , te bereken, te vergelyk en hulle toepaslikheid op CdTe te ondersoek.

Meeste van die metodes in gebruik om r_c te bereken geld vir goeie ohmiese kontakte. Die voorgestelde metode word aanbeveel om swak tot redelike ohmiese kontakte, gewoonlik die geval met ohmiese kontakte op CdTe, te evalueer.

INDEX

	Page
INTRODUCTION	1
I THEORY OF OHMIC CONTACTS	3
I-1 Formation of the metal–semiconductor contact	3
I-2 Characterizing an ohmic contact	7
I-3 Substrate surface properties	10
I-4 The interfacial layer	13
I-5 Studying the interfacial layer	14
I-5-1 The clean semiconductor surface	14
I-5-2 The dilute limit	15
I-5-3 Mono layer formation	16
I-5-4 Asymptotic overlayer	17
I-6 Ohmic contacts to wide–bandgap semiconductors	18
I-6-1 Material properties favorable for ohmic contacts	18
I-6-2 Material properties unfavorable for ohmic contacts	19
I-6-3 Techniques for improving contact ability	19
I-6-4 Systematics for contacts to CdTe	20
II METHODS OF MEASURING SPECIFIC CONTACT RESISTANCE	22
II-1 Introduction	22
II-2 Simple method	24
II-3 Spreading resistance method (Cox & Strack)	26
II-4 Method of Jaeger and Seipp	28

II-5	Method of Anthony et al	30
II-6	Transmission line method	33
II-7	Proposed method	37
II-8	Multi contact method	41
II-9	Comparison between the methods	43
III	METAL SYSTEMS ONTO CdTe	45
III-1	n-type CdTe	45
III-2	p-type CdTe	46
IV	EXPERIMENTAL PROCEDURE	47
IV-1	Preparation procedure	47
IV-2	Contact fabrication	47
IV-3	Method for measuring the specific contact resistance	49
IV-4	Auger electron spectroscopy	49
V	APPARATUS	53
VI	RESULTS AND DISCUSSION	55
	Part I Ohmic contacts to n-type CdTe	55
	Part II Ohmic contacts to p-type CdTe	65
	Part III Observations	76
V-II	CONCLUSION	84
	ACKNOWLEDGEMENTS	86
	REFERENCES	87

INTRODUCTION

Research and development efforts on cadmium telluride (CdTe) have been ongoing for many years. The application of CdTe ranges from solar cells [1,2] to sensors and detectors [3,4], the latter mainly X-ray and γ -ray devices. The ability to manufacture good ohmic contacts is of major importance to solar cells, while low leakage currents are essential in the application as detectors [5].

The metal contacting on such devices remains a serious problem which could be attributed to many factors including surface characteristics of the CdTe, barrier heights of the metal contacts and the difficulty to introduce dopant impurities in CdTe [1,2,5].

Characterization of ohmic contacts by determining the specific contact resistance has been done by a large number of researchers[6,7,8,9,10]. The range of specific contact resistance that can accurately be measured is only specified for a few methods. In many cases approximations have been made that are not applicable to the situation or not practical to implement.

The aim of this work is to investigate some of the different methods currently used for determining the specific contact resistance, r_c , and to establish a criteria to determine the range of r_c for which a particular method is accurate.

In order to test the validity of this criteria the most appropriate method will then be used to determine the specific contact resistance of indium (In) ohmic contacts on n-type CdTe, and a copper/gold (Cu/Au) alloy on p-type CdTe samples of different bulk resistivities.

This method will then be used for further studies pertaining to the characterization of ohmic contact manufacturing, of which the main objective is to investigate the different preparation and contacting procedures.

CHAPTER I. THEORY OF OHMIC CONTACTS.

I-1 FORMATION OF THE METAL-SEMICONDUCTOR CONTACT.

An ohmic contact can be defined as a metal-semiconductor contact with a linear relation between the current flowing through the contact and the potential drop across it. A good ohmic contact has a negligible contact resistance relative to the bulk resistance of the semiconductor.

The ideal ohmic contact on a n-type semiconductor is achieved by the formation of a metal-semiconductor contact between a metal of work function ϕ_m and a semiconductor of work function ϕ_s , with $\phi_s > \phi_m$. The work function of a metal is defined as the amount of energy required to raise an electron from the Fermi level to the vacuum level. The vacuum level is the energy level of an electron just outside the metal with zero kinetic energy and is the reference level in Fig. 1a. The work function ϕ_m has a volume contribution due to the periodic potential of the crystal lattice and a surface contribution due to the possible existence of a dipole layer at the surface [11]. The work function ϕ_s of the semiconductor is defined similarly and is a variable quantity due to the dependence of the Fermi level on doping. An important surface parameter which does not depend on doping is the electron affinity χ_s , defined as the energy difference of an electron between the vacuum level and the lower edge of the conduction band. The work functions ϕ_m and ϕ_s and the electron affinity are usually expressed in electron volt (eV).

The electron energy band diagrams for the above metal semiconductor are

given in Fig. 1. Figure 1a illustrates the energy bands for the separated materials. After the contact is fabricated electrons flow into the conduction band of the semiconductor, leaving behind a positive charge on the metal and causing an accumulation of electrons on the semiconductor side of the boundary. When equilibrium is reached the Fermi level in the semiconductor is raised by an amount $(\phi_s - \phi_m)$ as shown in Fig. 1b [11]. The accumulation charge in the semiconductor is confined to a thickness of the order of the Debye length and is essentially a surface charge. Since the concentration of electrons in the metal is very large, the positive charge on the metal side is also a surface charge contained within a distance of approximately 50 pm from the metal–semiconductor interface. It is clear that no depletion region is formed in the semiconductor and there is no potential barrier for the electron flow either from the semiconductor towards the metal or in the opposite direction. The electron concentration is increased in the region near the interface and the highest resistivity region in the system is the bulk semiconductor region. Practically all the externally applied voltage appears across this bulk region as shown in Figs. 1c and 1d for the two directions of current flow. It is thus obvious that the current is determined by the resistance of the bulk region and is independent of the direction of the applied bias. Such a non–rectifying contact is referred to as an ohmic contact.

A similar consideration can be used to show that, for a metal– p–type semiconductor contact, we also obtain an ideal ohmic contact if $\phi_m > \phi_s$.

A non–ideal but satisfactory ohmic contact should not significantly perturb device performance so that it can supply the required current with a

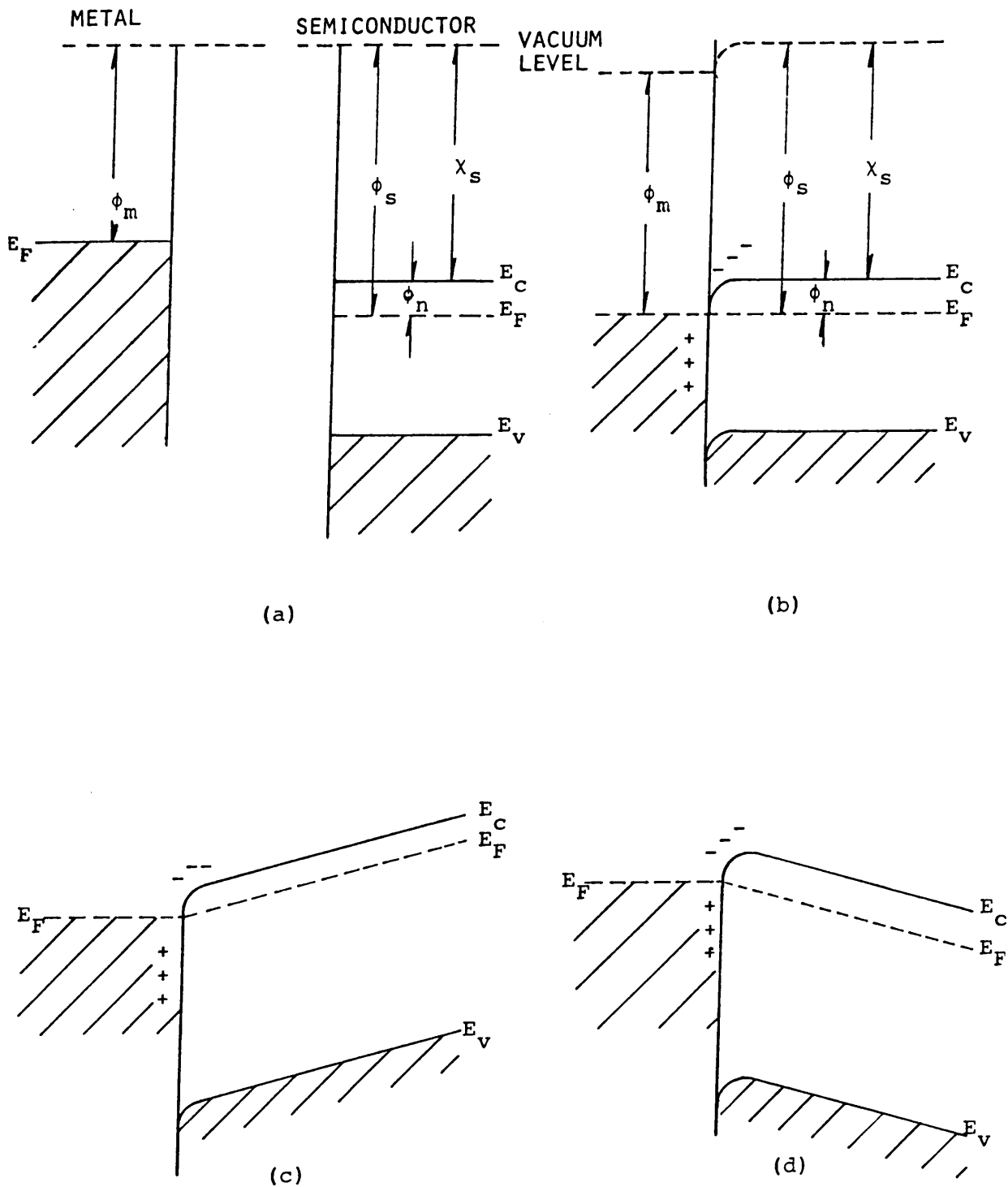


Fig. 1: Electron energy band diagrams of metal contact onto n-type semiconductor with $\phi_m < \phi_s$; (a) Neutral materials separated from each other, (b) contact under thermal equilibrium, (c) negative bias on the semiconductor, and (d) positive bias on the semiconductor. Figure obtained from reference 11.

sufficiently small potential drop across the contact when compared with that of the active region of the device. Using the above argument we can obtain an ohmic contact using a rectifying contact with a low barrier height so that thermionic-emission is the dominant current transport mechanism as shown in Fig. 2a. The second model is to obtain a barrier which is very narrow so that quantum mechanical tunneling is the dominant transport mechanism. This is obtained by high doping of the semiconductor below the contact as shown in Fig. 2b. With such a rectifying contact on a n-type semiconductor the metal work function ϕ_m will be larger than the semiconductor work function ϕ_s ($\phi_m > \phi_s$). For a p-type semiconductor it is clear that $\phi_s > \phi_m$.

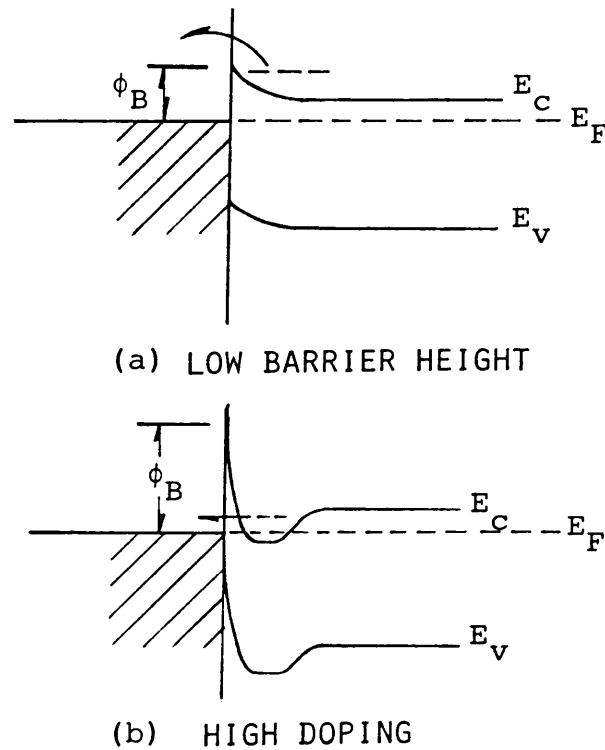


Fig. 2: Low barrier height and/or high doping ensures an ohmic contact on a n-type semiconductor if $\phi_m > \phi_s$ (non-ideal ohmic contact) this figure was obtained from reference 11.

I-2 CHARACTERIZING AN OHMIC CONTACT.

The first step in evaluating an ohmic contact is to establish whether the relation between the current flowing through it and the potential drop across it is linear as shown in Fig. 3.

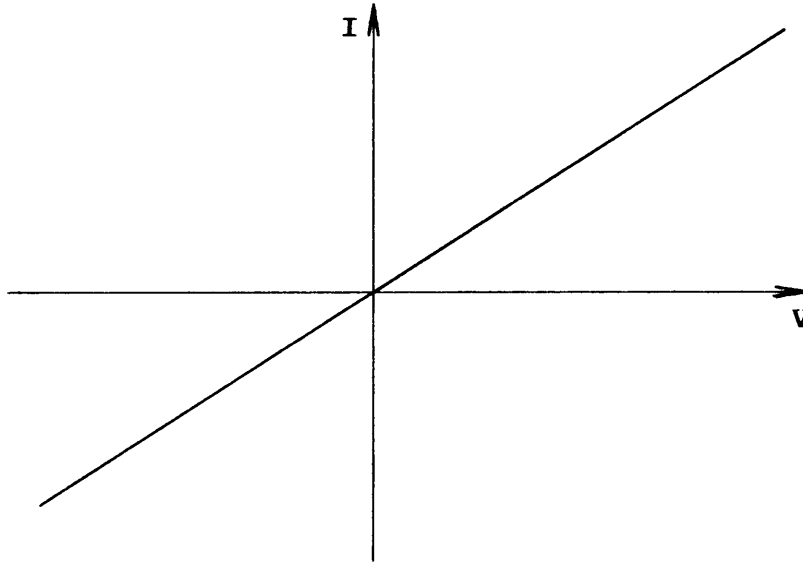


Fig. 3: If the current through the contact increases linearly with the potential drop across it, the contact is said to be ohmic.

After establishing that the contact is indeed ohmic we have to evaluate the quality of the contact by measuring the specific contact resistance r_c , which is defined as the product of the contact resistance R_c and the area A of the contact, with current flow perpendicular to the interface.

$$r_c = R_c A \quad \dots\dots\dots(I-201)$$

The contact resistance R_c is the resistance a contact offers to electrical current

through a metal–semiconductor interface and is only dependant on the nature of the interface and its area.

For a homogeneous contact the contact resistance R_c is defined as the ratio of the potential drop across the contact to the current flowing through it.

$$R_c = \frac{V}{I} \dots\dots\dots(I-202)$$

For a non–homogeneous contact the specific contact resistivity r_c is defined as the reciprocal of the derivative of current density with respect to voltage at zero biased voltage [11].

$$r_c = \left(\frac{\partial J}{\partial V}\right)^{-1} \Big|_{V=0} \dots\dots\dots(I-203)$$

In the case of a metal–semiconductor contact with low doping concentrations, the thermionic–emission current dominates the current transport and we have[11]

$$r_c = \frac{k}{qA^*T} \exp\left[\frac{q\phi_B}{kT}\right] \dots\dots\dots(I-204)$$

where A^* is the effective Richardson constant

$$A^* = \frac{4\pi qm^*k^2}{h^3} \dots\dots\dots(I-205)$$

and m^* is the effective mass of the charge carriers in the semiconductor, q the

charge of the carriers, k Boltzman's constant, h Plank's constant, ϕ_B the barrier height and T the temperature. Equation I-204 shows that a low barrier height should be used to obtain a low specific contact resistance r_c (Fig. 2 a).

For contacts with higher dopings, the tunneling current will dominate and we will have

$$r_c \propto \exp \left[\frac{2 \sqrt{\epsilon_s m^*} \phi_B}{h \sqrt{N_D}} \right] \dots\dots\dots(I-206)$$

where ϵ_s is the dielectric constant and N_D the doping level in the semiconductor. Equation I-206 shows that in the tunneling range the specific contact resistance r_c , strongly depends on the doping concentration (Fig. 2 b).

The specific contact resistance r_c is quoted in $\Omega.cm^2$. In this work ohmic contacts will be classified into three groups. The specific contact resistance is very much affected by the doping level of the CdTe. There exists a strong relation between the doping level in the CdTe and the bulk resistivity of the CdTe. Thus instead of relating the specific contact resistance to the doping level it will be related to the bulk resistivity, since this value is more than often supplied by the manufacturer.

For a CdTe sample with a bulk resistivity, ρ , of $10 \Omega \cdot \text{cm}$ the following classification will hold for r_c ;

- poor ohmic contact $r_c = 6 - 20 \Omega \cdot \text{cm}^2$
- moderate ohmic contact $r_c = 1 - 6 \Omega \cdot \text{cm}^2$
- good ohmic contact r_c below $1 \Omega \cdot \text{cm}^2$

To establish a rule of thumb that can be applied to CdTe, samples of different bulk resistivities (i.e. with different doping levels) the following classification will be used for r_c ;

- poor ohmic contact $r_c = 60\% - 200\%$ of the bulk resistivity
- moderate ohmic contact $r_c = 10\% - 60\%$ of the bulk resistivity
- good ohmic contact $r_c =$ below 10% of the bulk resistivity

When measuring R_c we usually measure the resistance R_T of a circuit containing for example, a semiconductor and two contacts where R_T is composed of:

- (a) The resistance of leads and meter R_o
- (b) The resistance of the contacts R_{c1} and R_{c2}
- (c) The resistance due to the semiconductor, bulk and spreading resistance R_s .

$$R_T = R_{c1} + R_{c2} + R_s + R_o \dots\dots\dots(I-207)$$

I-3 SUBSTRATE SURFACE PROPERTIES

The structure of the crystal determines the surface states of a material. The

CdTe crystal has a zincblende structure with a lattice constant $a_0 = 6,482 \text{ \AA}$ at 300 K.

The interfaces between metals and semiconductors have been classified into four types according to the resulting interfacial atomic configuration [12] as listed below;

Type 1 The semiconductor is very much like an insulator and the metal is physisorbed on its surface.

Type 2 The semiconductor is highly polarizable ($\epsilon_s > 7$) [8] and the metal forms a weak chemical bond but does react with it to form a bulk compound.

Type 3 The highly polarizable semiconductor reacts with the metal and forms one or more chemical compounds.

Type 4 A thin film of native elements deposited during the surface preparation of the highly polarizable semiconductor prevents an intimate contact between the metal and the semiconductor. The film is referred to as an interfacial layer.

Type 1 interface is an ideal Schottky barrier contact in which the barrier height varies directly with the metal work function. This type of interface is also ideal for ohmic contacts, since by choosing a metal with the correct work function we can obtain a low barrier and equation I-204 can be used to calculate the specific contact resistance r_c .

Type 2 approximates to a "Bardeen barrier" provided that the surface states are assumed to be distributed in space inside the semiconductor to allow a potential drop across this region [13]. In the clean contacts of this type one would expect the barrier height to show a weak dependence on ϕ_m . This type of interface could also be used as an ohmic contact since the barrier height is lowered by the surface states and is given by

$$\phi_B(m,s) = S(s) X_m + \phi_0(s) \quad \dots\dots\dots(I-302)$$

where m and s refer to the metal and the semiconductor, respectively, $\phi_0(s)$ represents the contribution of the surface states and the interface index $S(s) = \frac{d\phi_B}{dX_m}$ gives the dependence of barrier height on the metal electronegativity. For covalently bonded materials S is nearly zero and ϕ_B is substantially independent of X_m . Ionic semiconductors on the other hand have large values of S and the value of ϕ_B increases linearly with X_m [11]. Kurtin et al [14] have suggested that S is a function of the electronegativity difference $\Delta X = X_A - X_m$ in the semiconductor, which is a measure of the ionicity of the material [11].

Type 3 interface represents a case of strong chemical bonding between the metal and the semiconductor and hence we would expect the barrier height to depend on some quantity related to chemical or metallurgical reactions at the interface.

A type 4 contact is the one which is most frequently encountered in actual metal semiconductor devices.

Ohmic contacts to CdTe are mainly of type 2 and 4 [15].

Many factors determine the interfacial composition, width and the number of states.

The interface can be analyzed by making use of the layer-by-layer method of fabrication. Interrupting the development at a given point and then studying the interface before depositing more material. The metal thickness dependence of the barrier evolution and the substantial changes that take place at various stages of the interface formation [16] should be kept in mind.

The state of the semiconductor surface will affect the metal-semiconductor contact that forms after the preparation of the clean surface. This state can consist of either structural or compositional disorders reflected in structural defects which can generate surface states [17,18].

On starting metal deposition, the density of surface atoms are sufficiently low that they do not interact. Here one can identify site-specific chemisorption as well as reaction or replacement. Energy such as heat of condensation or reaction may dislodge other surface atoms from their equilibrium sites.

As the concentration of metal grows on the surface, the probability of metal-metal interactions becomes more significant. The tendency for the metal to form clusters is determined by surface mobility and the strength of interactions. For many metals this cluster formation is exothermic, and can disrupt the underlying lattice.

After the formation of the initial metal overlayer, the metal film may be under a significant stress, which can be a driving force for interdiffusion and at some point, dislocation formation. The final interface may be compositionally and spatially inhomogeneous.

I-5 STUDYING THE INTERFACIAL LAYER.

Interface formation can be studied at the following stages;

- (1) Clean semiconductor surface.
- (2) Dilute limit of metal deposition.
- (3) Metal nucleation.
- (4) Asymptotic overlayer.

The interface layer can have a multiplicity of zones with a division between metallic and semiconducting regions. Generally there are two zones on the semiconductor side and a similar division on the metal side. Each of these stages can influence the quality of a metal semiconductor contact. Stage 1 and 4 will be investigated using Auger electron spectroscopy.

I-5-1 State 1: The clean semiconductor surface.

Clean semiconductor surfaces can be divided into two cases, the ordered and disordered. In cleaved surfaces, disordering usually results from structural damage induced by cleaving. Surfaces cleaned by a sputtering technique [19] usually results in the surface becoming disordered and in the case of compound semiconductors, nonstoichiometric, which can usually be restored by annealing.

Most vacuum–semiconductor interfaces reconstruct so that they exhibit lateral periodicities or coordinates different from a strict truncation of the lattice [20–22]. This reconstruction has an influence on the character of surface states, which are very sensitive to the presence of adsorbates or overlayers. The unreconstructed bulk terminated structures for three low index planes of a zincblende lattice are shown in fig. 4. The behavior for adatoms deposited onto these surfaces will most probably differ.

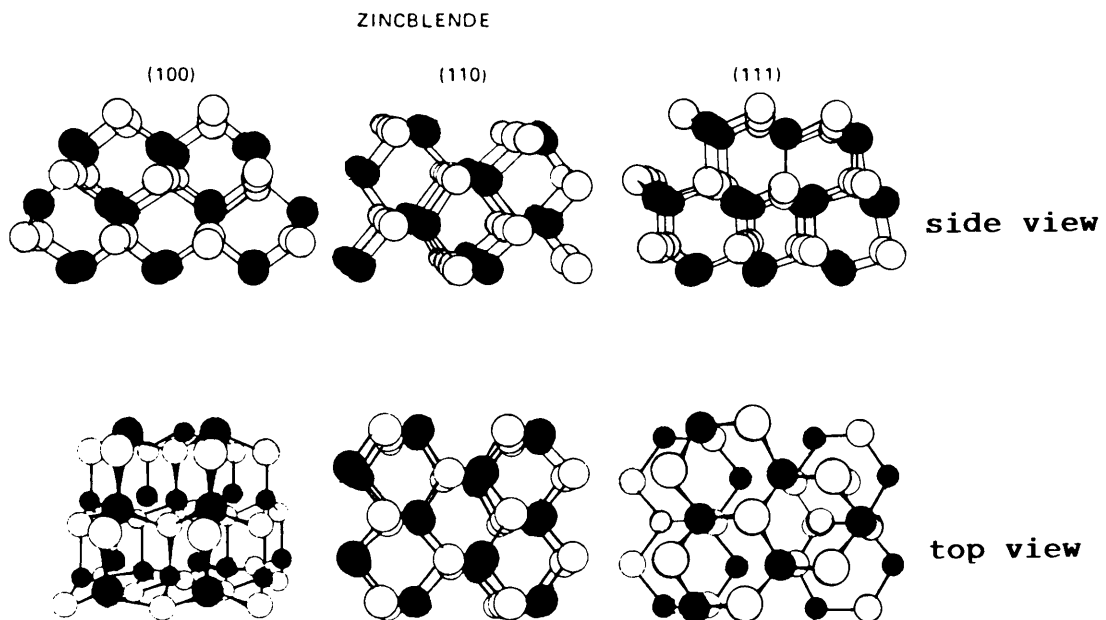


Fig. 4: Unreconstructed representations of low index zincblende surface structures[11].

I–5–2 Stage 2: The dilute limit.

This is the initial stage of interface development and has a density of adatoms small enough that a continuous metal film does not form. "Where then does a metal atom sit when deposited on a clean semiconductor surface?" A metal

atom may be strongly bound to the surface and in many cases the atoms have considerable lateral mobility. As the concentration of metal increases it may lead to metal cluster formation well below a thickness of half a mono layer. Some atoms may find sites beneath the semiconductor surface.

The structural character of the dilute limit depends strongly on the surface and temperature of the semiconductor during deposition. An important factor of the dilute limit is that the heat of condensation of the metal atom may be sufficient to dislodge semiconductor surface atoms.

Additional metal that is added causes a transformation in the nature of the states.

I-5-3 Stage 3: Mono layer formation.

The most important part in determining the character of the interface is the formation of the first few metal mono layers.

Inter diffusion starts due to the heat released as the metal nucleates to form a mono layer. The deposition temperature and subsequent annealing determine the structural character of the mono layer. The Fermi-level pinning is mostly complete once the first mono layer of metal is established. The increase in metal density during this stage is also likely to affect the character of interfacial defects created during stage 2.

Studies have shown that many aspects of the interface are sensitive to the ordering of metal at this stage. Studies by Kleinman et al [23] have found

that three mono layers are generally required to converge to metallic like properties.

I-5-4 Stage 4:Asymptotic overlayer.

The final character of the interface can continue to change as additional mono layers are added. Strain fields due to lattice mismatch and grain boundary phenomena can play an important role.

Increased temperatures or bias conditions can accelerate inter diffusion and often make interfaces metastable.

An overriding fact of metal–semiconductor interfaces is the intrinsic aspects of interfacial inter diffusion and interaction. The inter diffusion can result in interface layers with radically different characteristics from the supposed components.

The asymptotic interface, which may be homogeneous or inhomogeneous, results when additional deposition does not appreciably change the composition or doping of either the deposited metal or the semiconductor.

It may also depend on the annealing history. Time versus temperature is important both from the point of view of diffusion and from activation energies for reaction.

I-6 OHMIC CONTACTS TO WIDE-BANDGAP
SEMICONDUCTORS

I-6-1 Material properties favorable for ohmic contacts.

There are several groups of wide-bandgap semiconductors whose material properties make their contacting fairly straightforward.

- (1) If a semiconductor is required to have a high carrier concentration and can be doped heavily without difficulties in the area just below the contact, it is of little consequence whether the contacting material forms a barrier or not. This heavy doping results in a narrow barrier and tunneling of carriers through the barrier will dominate the transport of carriers.

A high carrier concentration can be achieved by the techniques of alloy regrowth, diffusing in a dopant or by ion implantation.

- (2) The conductivity is influenced by the ambient atmosphere during the heating cycle to which they are subjected during the process of contact manufacturing. Metals having a strong affinity for oxygen lead to ohmic contacts on n-type material, while the best ohmic contacts on p-type materials are obtained with metals like gold, platinum and palladium in oxygen atmosphere [24].

I-6-2 Material properties unfavorable for ohmic contacts.

- (1) Wide-bandgap semiconductors which present contacting problems because they cannot be doped heavily enough.
- (2) Chemically unstable materials or compounds which undergo a chemical conversion to a different compound upon heating, and degrade the quality of the contacts.

I-6-3 Techniques for improving the quality of ohmic contacts.

There are cases where there is difficulty in obtaining an ohmic contact due either to unsuitable work function matching or heavy doping beneath the contact, but techniques exist which can improve contact quality.

- (1) The bandgap, electron affinity, or the nature of the surface states of the semiconductor near the surface can be changed by forming a mixed crystal of a given semiconductor with another one similar in nature, but having a more favorable bandgap, electron affinity, electronegativity or set of surface states [11].

For example, on p-type CdTe, due to the better ohmic contact quality on $\text{Zn}_x\text{Cd}_{1-x}\text{Te}$, as compared with pure cadmium telluride, a solid solution between CdTe and ZnTe is formed on the surface of p-type CdTe [25].

- (2) It may be possible to achieve a metallographic micro structure

under the contact which creates a multitude of sharp spikes. At the tip of each spike there is a very high field gradient, which promotes injection of charge carriers. The contact as a whole behaves like an ohmic contact since the total voltage drop at each spike is small and the large number of spikes of different geometry, orientation and field gradient.

I-6-4 Systematics of contacts to Cadmium Telluride.

The general principles that can be applied to CdTe will now be discussed.

First examine the applicability of the electron affinity – work function match principle. When two surfaces are brought together it is assumed that there is no net change in surface dipole layers as a result of contact. Models to predict the interface barrier height on metal work function and semiconductor electron affinities exists. A guide to select the appropriate model has been suggested by Mead [26].

Mead predicts that surface states play a dominant role in stabilizing the Fermi-level near the middle of the band gap in materials with dominantly covalent bonding. In ionic materials, as is the case with CdTe, the surface states move toward the band edges in proportion to the ionic contribution to the binding energy and play a lesser role in fixing the position of the Fermi-level at the surface. Since II-VI compounds are quite ionic semiconductors, we may expect the simple model without surface states to be most applicable to these materials.

CdTe has an electron affinity of 4.3 eV. On n-type CdTe gallium and indium with work functions close to or below this figure should be good contact materials. It was experimentally found that if care is taken not to overheat the CdTe crystal during or after contact manufacture, the Mead model predicts that indium contacts should stay ohmic down to temperatures below the liquid hydrogen range and free carrier densities of less than 10^{11} cm^{-3} [15].

The sum of the band gap and the electron affinity in CdTe is 5.8 eV. On p-type CdTe the Fermi-level of gold does not reach below or even close to the valence band edge, but is still within reach at higher temperatures (at room temperature gold makes a satisfactory ohmic contact on p-type CdTe).

Better results are obtained by the technique of alloying CdTe and ZnTe on the surface of CdTe before the contact is formed [25].

CHAPTER II METHODS OF MEASURING r_c

II-1 INTRODUCTION

The current flow patterns and the spreading effects of all systems are not the same. For a radial system as in Fig. 5 it can be shown that the spreading resistance for a circular disc of radius a is given by

$$R_s = \frac{\rho}{4a} \quad \dots\dots\dots(\text{II-101})$$

where ρ is the bulk resistivity of the semiconductor [27].

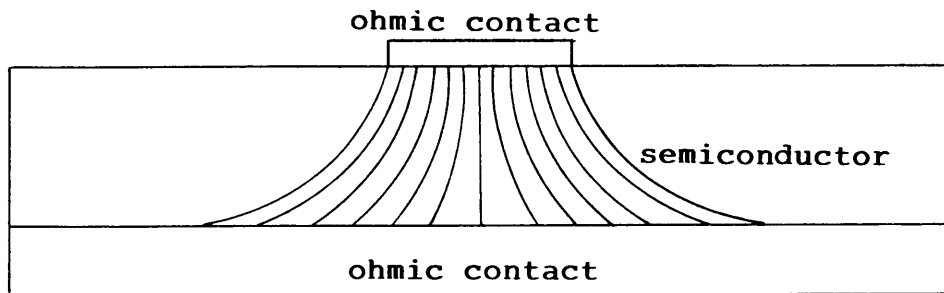


Fig. 5 The current flow patterns in a radial system.

With most modern systems where contacts are made on a small scale a planar current flow pattern as in Fig. 6 is present and the shape of the contact influences the spreading effects.

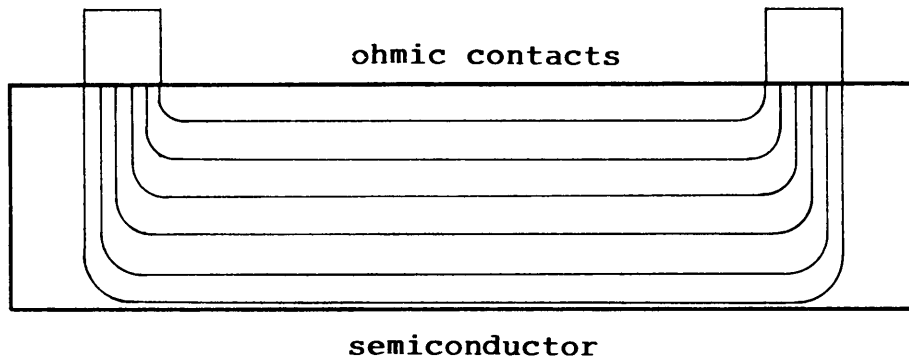


Fig. 6 Current flow patterns for a planar system

There are two methods for analyzing such systems. The first is an approach as explained by Hall, and Tiny and Chen [28,29], based on a conformal transformation of the prevailing electrode geometry into a geometry for which the solution is obvious. This method has been applied to a great variety of electrode shapes [30].

The second method considers the spreading resistance as a lossy transmission line with lumped components [31–34]. This method leads to an approximation, but is more often entirely adequate.

This chapter will deal with some methods for measuring the specific contact resistance and supply a criteria to determine an upper and lower limit for the specific contact resistance r_c that could be measured accurately with the method.

II-2 SIMPLE METHOD

With this method each side of the semiconductor is covered by a metal contact as in Fig. 7. By passing a current between the two metal–semiconductor contacts separated by a 'sandwich' of semiconductor of resistivity ρ .

The total resistance R_T measured is given by I-207, $R_T = 2R_c + R_s + R_o$, and can be written as

$$R_T = \frac{2r_c}{A} + \frac{\rho d}{A} + R_o \quad \dots\dots\dots(\text{II-201})$$

where A is the area of the contacts, R_o the circuit resistance and d the thickness of the semiconductor.

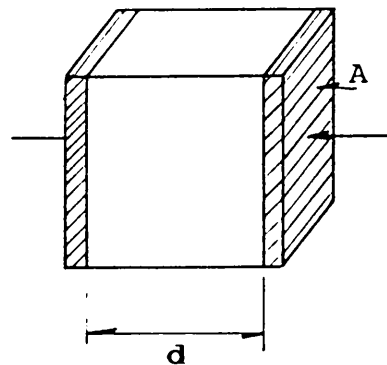


Fig. 7: 'Sandwich' of semiconductor between two ohmic contacts of area A .

An accurate value of r_c can only be measured if

$$\frac{2r_c}{A} \simeq \frac{\rho d}{A} + R_o \quad \dots\dots\dots(\text{II-202})$$

otherwise the one term would overshadow the other. If the one term is 10 times the other, r_c could still reasonably accurately be determined. Using this criteria we can obtain a lower limit for r_c as

$$r_{c_{\text{lower}}} = \frac{\rho d}{20} + \frac{R_o A}{20} \quad \dots\dots\dots(\text{II-203})$$

and an upper limit given by

$$r_{c_{\text{upper}}} = 5\rho d + 5R_o A \quad \dots\dots\dots(\text{II-204})$$

As an example, if $\rho = 10 \Omega.\text{cm}$, thickness $d = 400 \mu\text{m}$, area $A = 8 \times 10^{-4} \text{cm}^2$ and the circuit resistance $R_o = 2 \Omega$, typical lower and upper values found for CdTe are:

$$\begin{aligned} r_{c_{\text{lower}}} &= 2.0 \times 10^{-2} \Omega.\text{cm}^2 \\ r_{c_{\text{upper}}} &= 2.0 \Omega.\text{cm}^2 \end{aligned}$$

This gives a fair range of values for r_c that can accurately be measured if the contact is of moderate quality. Many ohmic contacts on CdTe have a value of $r_c > \rho$, and in such cases this method will be insufficient. The specific contact resistance is related to the bulk resistivity as explained in paragraph I-2. On the other hand if the quality of the ohmic contact is very good this method will also not suffice.

II-3 SPREADING RESISTANCE METHOD (Cox and Strack)

This method makes use of a number of ohmic contacts of different sizes on the one side of the semiconductor surface. The other surface is entirely covered with an ohmic contact as shown in Fig. 8.

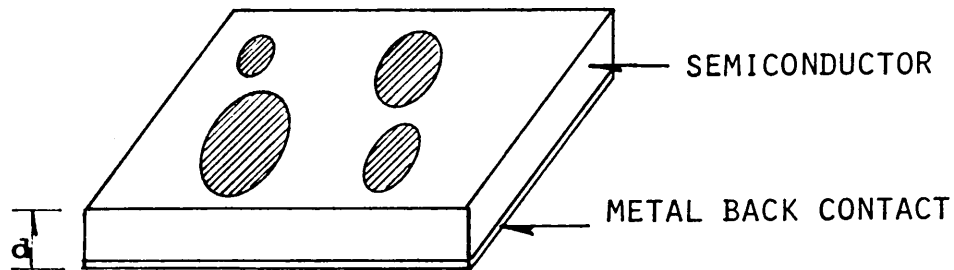


Fig. 8: The configuration used by the spreading resistance method.

The resistance between any ohmic contact and the ohmic contact on the bottom of the semiconductor is a function of the area of the contact and is given by equation I-207, $R_T = R_c + R_s + R_o$, which can be written as [6].

$$R_T = \frac{r_c}{\pi a^2} + \frac{\rho}{2\pi a} \arctan \left[\frac{2d}{a} \right] + R_o \dots(\text{II-301})$$

where ρ is the bulk resistivity of the semiconductor, R_o the circuit resistance defined in I-207, d the thickness of the semiconductor, and a the radius of the ohmic contact.

For samples where $2d \gg a$ so that $\arctan \left[\frac{2d}{a} \right] \simeq \frac{\pi}{2}$ we can approximate

equation II-301 by

$$R_T = \frac{r_c}{\pi a^2} + \frac{\rho}{4a} + R_O \dots\dots\dots(\text{II-302})$$

Many cases arise with samples where $2d \simeq a$, and $\arctan \left[\frac{2d}{a} \right] \simeq \frac{\pi}{4}$. By substituting this in equation II-301 gives

$$R_T = \frac{r_c}{\pi a^2} + \frac{\rho}{8a} + R_O \dots\dots\dots(\text{II-303})$$

If the value of ρ and R_O are unknown, the value of r_c can be obtained by fitting the best curve to a plot of R_T versus $\frac{1}{a}$. If the values of ρ and R_O are known the value of r_c can be obtained directly from equation II-301.

Using the same criteria as in section II-2 an accurate value of r_c can only be obtained if

$$\frac{r_c}{\pi a^2} \simeq \frac{\rho}{2\pi a} \arctan \left[\frac{2d}{a} \right] + R_O \dots\dots\dots(\text{II-304})$$

A lower limit for the value of r_c is then given by

$$r_{c_{\text{lower}}} = \frac{\rho a}{20} \arctan \left[\frac{2d}{a} \right] + \frac{R_O \pi a^2}{10} \quad (\text{II-305})$$

and an upper value given by

$$r_{c_{\text{upper}}} = 5\rho a \arctan \left[\frac{2d}{a} \right] + 10R_o \pi a^2 \quad (\text{II-306})$$

Using the same data as in section II-2 to obtain lower and upper values we find

$$\begin{aligned} r_{c_{\text{lower}}} &= 1.1 \times 10^{-2} \Omega \cdot \text{cm}^2 \\ r_{c_{\text{upper}}} &= 1.1 \Omega \cdot \text{cm}^2 \end{aligned}$$

For a good ohmic contact(as defined in paragraph I-2) we find that this method is adequate. This method allows the measurement of a reasonable high value of r_c .

II-4 METHOD OF JAEGER AND SEIPP

This method employs a planar current flow pattern between two identical ohmic contacts on the same side of the semiconductor as in Fig. 9. The resistance R_T between these two contacts is a function of the radius of the contacts, bulk resistivity of the semiconductor and the specific contact resistance and is given by I-207, $R_T = 2R_c + R_s + R_o$, which can be written as [7].

$$R_T = \frac{2r_c}{\pi a^2} + \frac{\rho}{2a} + R_o \quad \dots\dots\dots(\text{II-401})$$

if $a \ll d$, where a is the diameter of the two contacts and d the thickness of the sample.

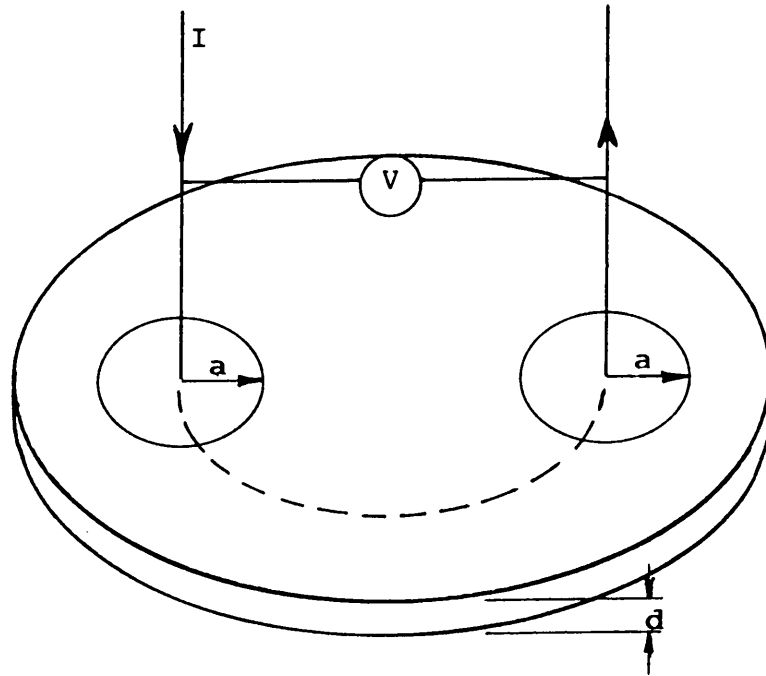


Fig. 9: The contact configuration as used with the method as explained by Jaeger and Seipp[7].

Measuring the value of R_T and knowing the values of ρ , a and R_0 the value of r_c can be calculated directly from equation II-401.

The accuracy range of this method can be established using the criteria in section II-2. An accurate value of r_c may be obtained if

$$\frac{2r_c}{\pi a^2} \approx \frac{\rho}{2a} + R_0 \quad \dots\dots\dots(\text{II-402})$$

The lower and upper values of r_c can then be calculated using

$$r_{c_{\text{lower}}} = \frac{\pi a \rho}{40} + \frac{R_o \pi a^2}{20} \dots\dots\dots(\text{II-403})$$

$$r_{c_{\text{upper}}} = \frac{5\pi a \rho}{2} + 5\pi a^2 R_o \dots\dots\dots(\text{II-404})$$

Using the same data as in section II-2 for an example we have

$$r_{c_{\text{lower}}} = 1.3 \times 10^{-2} \Omega.\text{cm}^2$$

$$r_{c_{\text{upper}}} = 1.3 \Omega.\text{cm}^2$$

For a good ohmic contact(as defined in paragraph I-2) this method should be adequate, but reasonably inadequate for a poor ohmic contact.

II-5 METHOD OF ANTHONY, FAHRENBRUCH AND BUBE

With this method, two identical contacts with a smaller contact between them are manufactured on the one side of the semiconductor. The other side is covered with multiple dot contacts as shown in Fig. 10.

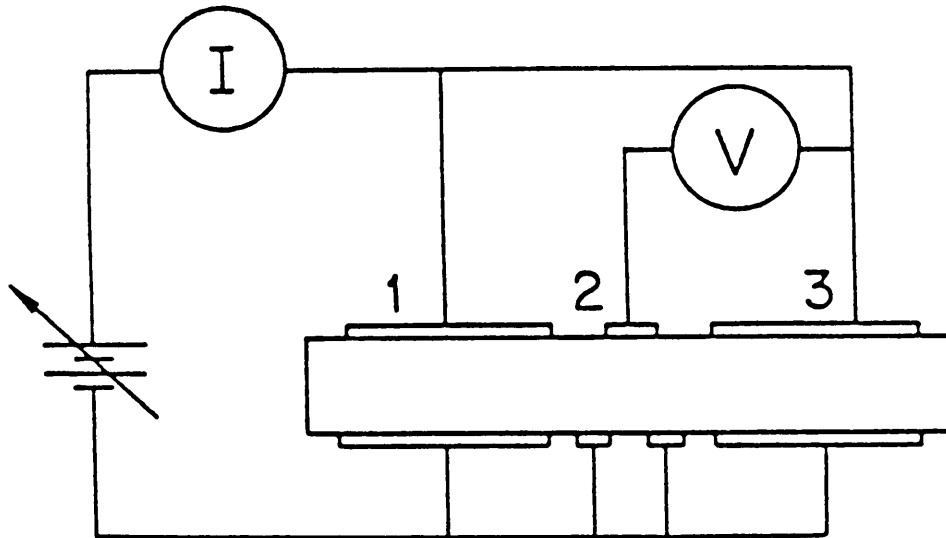


Fig. 10. The experimental setup of the contact as employed by the method of Anthony et. al[8].

The definition of specific contact resistance is used to determine its value [8]

$$r_c = \left[\frac{dJ}{dV} \right]^{-1} \Big|_{V=0} = A_c \left[\frac{dI}{dV} \right]^{-1} \Big|_{V=0} \dots(\text{II-501})$$

where I is the current, V the voltage as measured in Fig.10 and A_c the area of the two identical contacts.

The assumption on which this method is based is that equipotential surfaces lie immediately beneath contacts 1, 2 and 3. This assumption is supported by Montgomery [35]. This implies that the voltmeter in Fig. 10 is measuring the potential difference between a point just below the metal/CdTe interface and a point just above the metal/CdTe interface.

Note that the circuit used to measure the resistance is measuring the combined resistance of contact 1 and 3. For this circuit equation II-501 must be changed to

$$r_c = \frac{A_c}{2} \left[\frac{dI}{dV} \right]^{-1} \Big|_{V=0} \dots\dots\dots(\text{II-502})$$

The advantage of this method is that a knowledge of the substrate material bulk resistivity is not required, no geometrical measurements are needed other than contact area, and the I-V characteristics are generated directly.

The accuracy of this method will strongly depend on the input impedance of the voltmeter used to measure the potential difference. In cases where the $R_i \simeq R_c$, where R_i is the input impedance of the voltmeter and R_c the contact resistance, the current measured will be divided into three parts instead of the correct two, which will result in an incorrect value of R_c , and hence r_c . The ideal will be when $R_i \gg R_c$. Assuming that when $R_i = 1000 R_c$ is an adequate condition to obtain an accurate value of r_c , we can find an upper limit for r_c that could still be measured accurately as

$$r_{c_{\text{upper}}} = \frac{R_i A}{1000} \dots\dots\dots(\text{II-503})$$

Using the test data as in II-2 and a voltmeter with an input impedance of $R_i = 11 \text{ M}\Omega$ (typical for laboratory instruments) we find an upper limit for r_c as

$$r_{c_{\text{upper}}} = 8.8 \Omega.\text{cm}^2$$

Applying this criteria to the data of Nazaki and Milnes [36] a voltmeter having an input impedance $R_i = 344 \text{ M}\Omega$ had to be used to obtain an accurate value $r_c = 5.5 \times 10^3 \Omega.\text{cm}^2$.

The lower limit for measuring an accurate value of the specific contact resistance will be determined by the sensitivity of the meters used. The largest change in current that can be measured with the apparatus is $1 \times 10^{-3} \text{ A}$ and the smallest step in the potential is $1 \times 10^{-2} \text{ V}$. This yields a gradient of 10 V/A for the graph of voltage as a function of current. Using the area of the contact as $8 \times 10^{-4} \text{ cm}^2$ we have that

$$r_{c_{\text{lower}}} = 4 \times 10^{-3} \Omega.\text{cm}^2$$

This method for measuring the specific contact resistance is limited by the area of the contacts and the input impedance of the voltmeter used in the circuit. This area dependence restricts the use of this method to determine the specific contact resistance on samples with high values of r_c .

II-6 TRANSMISSION LINE (LADDER NETWORK) METHOD.

This method for measuring the specific contact resistance uses a ladder structure as in Fig. 11 and was proposed by Schockley in 1964.

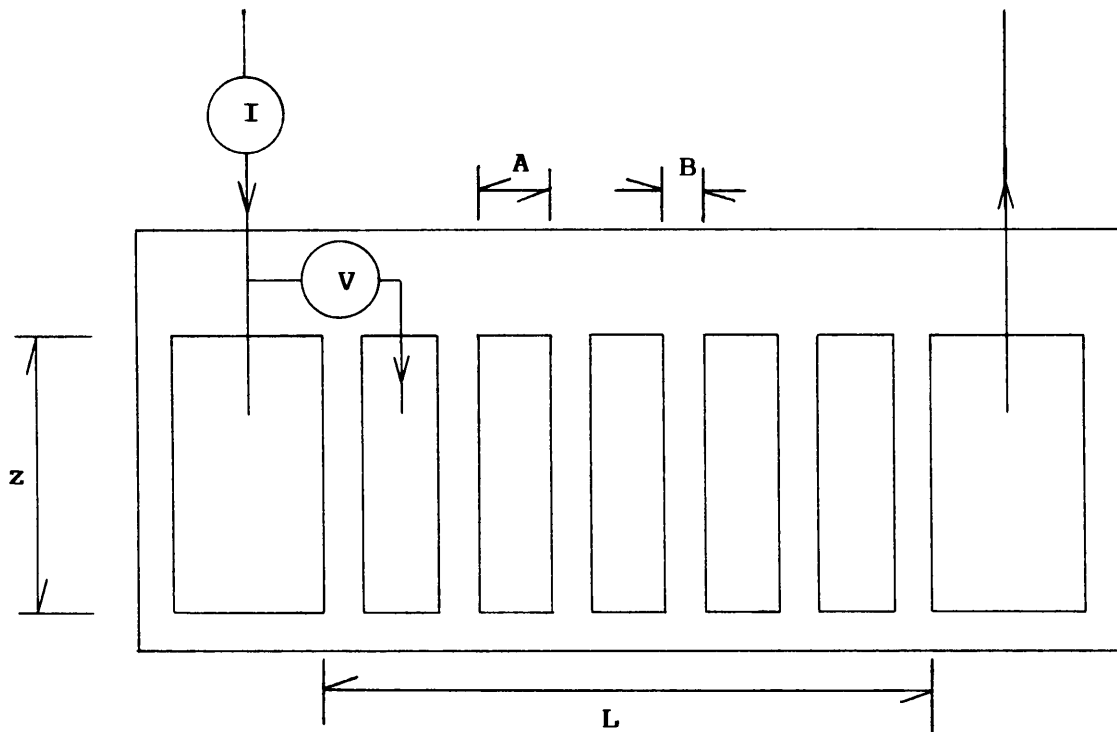


Fig. 11. Ladder network as used with the transmission line method to determine the specific contact resistance.

In this method a current I is flowing between two large-area ohmic contacts through a rectangular conducting sheet of semiconductor material. A high impedance voltmeter is used to measure the potential difference between one of these large-area ohmic contacts and each of a series of evenly spaced narrow ohmic contacts formed at right angles to the direction of current flow. A graph of potential against position can be drawn, and extrapolated to zero potential difference. Zero potential difference will not occur at the edge of the ohmic contact, but some distance L_t (transfer length) beyond it. The lower the value of L_t the lower the specific contact resistance will be. The specific contact resistance is determined from L_t and is given by [9]

$$r_c = L_t^2 R \quad \dots\dots\dots(\text{II-601})$$

where

$$R = \frac{V_{\text{app}} z}{I L} \quad \dots\dots\dots(\text{II-602})$$

Using the assumption $L_t > \frac{3A}{2}$ ensuring that r_c can be measured accurately the relation between the potential and position is given by[9]

$$V_n = \frac{IR}{z} x_n + \frac{IR}{z} L_t \quad \dots\dots\dots(\text{II-603})$$

The value of L_t is obtained from the x-intercept and R from the slope of the graph of potential against position.

When the width W of the stripe contacts become comparable with the transfer length L_t the accuracy of this method becomes questionable. For cases where $L_t \geq \frac{3}{2} W$ the specific contact resistance can still be measured accurately. The lower limit for an accurate measurement of r_c is then given by[9]

$$r_{c_{\text{lower}}} = \frac{\rho W^2}{4 d} \quad \dots\dots\dots(\text{II-604})$$

where ρ is the bulk resistivity and d the thickness of the semiconductor.

Using the test data as in II-2, and the width of the pick-off strips $W = 10 \mu\text{m}$ an example for a lower value for r_c is obtained

$$r_{c_{\text{lower}}} = 6.3 \times 10^{-5} \Omega.\text{cm}^2$$

For cases where $L_t < \frac{3}{2} W$ the method of variable gap as in Fig. 12 will be more accurate.

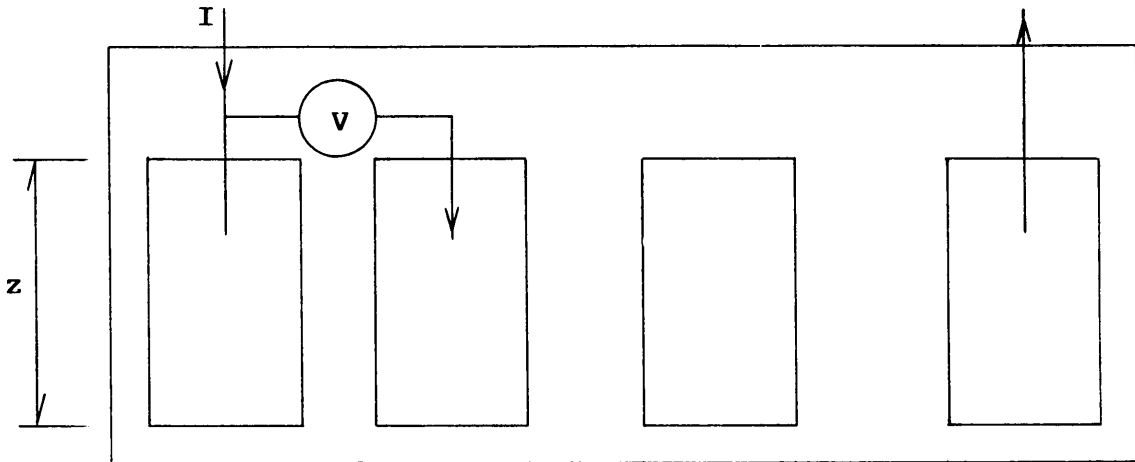


Fig. 12. The contact setup as used with the variable gap structure.

With this setup we have a number of large-area ohmic contacts spaced by different, known distances. Using a high impedance voltmeter the potential difference across each gap is measured. From this data a graph of potential difference against gap length can be plotted and extrapolated to zero potential and the value of L_t obtained. Note here the x-intercept will give $2L_t$ [9].

The upper limit for an accurate value of specific contact resistance will be determined by the ratio of the contact resistance R_c to the input impedance R_i of the voltmeter. When $R_c \simeq R_i$ then an error will be observed in the potential difference and an error in the calculation of L_t . Since $r_c \propto L_t^2$ and $r_c \propto R$, a much larger error will be detected in the value of r_c .

$$r_{c_{\text{upper}}} = 1 \times 10^{-2} \Omega \cdot \text{cm}^2$$

This method is thus not recommended for measurements of large values of specific contact resistance.

II-7 PROPOSED METHOD.

The total resistance R_t measured between two ohmic contacts on one side of a semiconductor is given by I-207 and can be written as

$$R_t = 2R_c + 2R_s + R_b + R_o \dots\dots\dots(\text{II-701})$$

when two identical contacts are used and R_b is the resistance contribution due to the bulk semiconductor between the two ohmic contacts. Each term in II-701 will now be discussed separately.

The contact resistance term R_c for a circular contact of radius a is given by

$$R_c = \frac{r_c}{\pi a^2} \dots\dots\dots(\text{II-702})$$

The spreading resistance term is determined by the type of current flow pattern that is present. For the setup as in Fig. 13 the current flow pattern is of a planar type as depicted in Fig. 5.

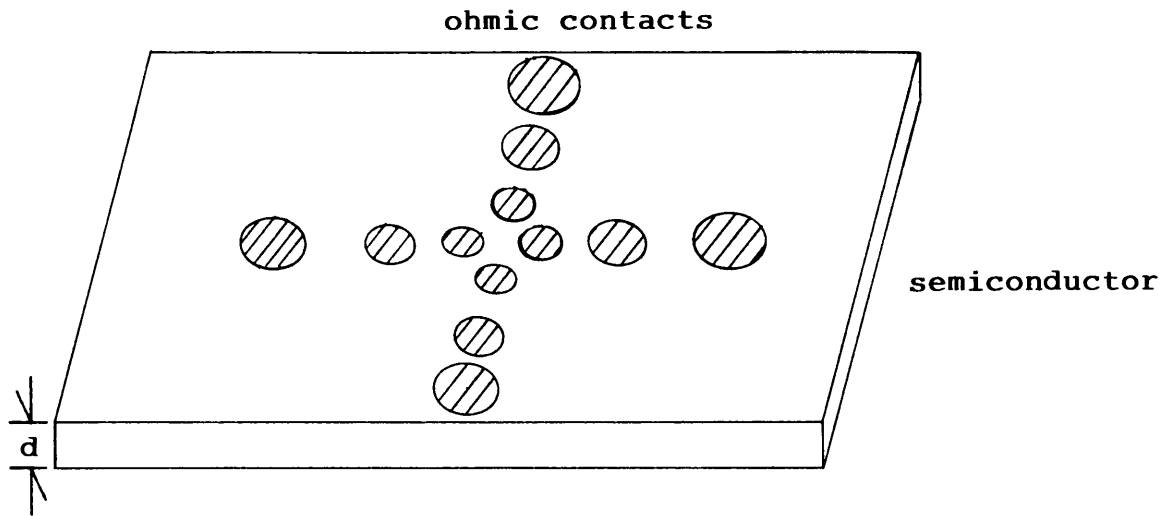


Fig. 13. Contact configuration as used in the proposed method.

The spreading resistance R_c for a square contact with sides W is given by

$$R_s = \frac{\rho}{W} \coth \left[\frac{W}{d} \right] \dots\dots\dots(\text{II-703})$$

where d is the thickness of the semiconductor sample [27]. Equation II-703 was derived by considering the current density from the ohmic contact. This equation can then be applied to a circular ohmic contact by substituting $1.77a$ as the value of W , since that will be the value of W for a square having the same area as a circle of radius a . For a circular contact II-703 will become

$$R_s = \frac{\rho}{1.77a} \coth \left[\frac{1.77a}{d} \right] \dots\dots\dots(\text{II-704})$$

The bulk resistance term depends strongly on the thickness of the semiconductor and the distance ℓ between the ohmic contacts and is given by

$$R_b = \frac{\rho \ell}{Wd} \quad \dots\dots\dots(\text{II-705})$$

and for a circular ohmic contact of radius a

$$R_b = \frac{\rho \ell}{1.77ad} \quad \dots\dots\dots(\text{II-706})$$

Substituting these terms into II-701 we have

$$R_t = \frac{2r_c}{\pi a} + \frac{2\rho}{1.77a} \coth \left[\frac{1.77a}{d} \right] + \frac{\rho \ell}{1.77ad} + R_o$$

$$R_t = \frac{2r_c}{\pi a} + \frac{\rho}{1.77a} \left[\frac{\ell}{d} + 2\coth \left[\frac{1.77a}{d} \right] \right] + R_o \quad (\text{II-707})$$

With this method a number of ohmic contacts having different, but known, radii and spacings are deposited onto one side of the semiconductor sample by the use of a mechanical mask. A graph of current against potential difference for each set of contacts is plotted from the slope of this graph the value of R_t is calculated. Since more than one value for r_c is obtained on one sample an average can be calculated.

The accuracy of calculating the specific contact resistance is determined by the ratio of contact resistance $2R_c$ to spreading resistance $2R_s$, bulk resistance R_b and circuit resistance R_o . For an accurate calculation of r_c we must have

$$2R_c \simeq 2R_s + R_b + R_o \quad \dots\dots\dots(\text{II-708})$$

By using the same criteria as in II-2 we find a lower and upper value for the specific contact resistance r_c that can be accurately calculated by

$$r_{c_{\text{lower}}} = \frac{\pi a \rho}{35.40} \left[\frac{\ell}{d} + 2 \coth \left[\frac{1.77a}{d} \right] \right] + \frac{\pi a^2}{20} R_o \quad (\text{II-709})$$

and

$$r_{c_{\text{upper}}} = \frac{5\pi a \rho}{1.77} \left[\frac{\ell}{d} + 2 \coth \left[\frac{1.77a}{d} \right] \right] + 5\pi a^2 R_o \quad (\text{II-710})$$

The test data as in II-2 gives a lower limit for r_c of

$$r_{c_{\text{lower}}} = 1.0 \times 10^{-1} \Omega \cdot \text{cm}^2$$

and an upper limit of

$$r_{c_{\text{upper}}} = 10.0 \Omega \cdot \text{cm}^2$$

when the separation between the contacts is 1.6 mm and $R_o = 2 \Omega$.

A disadvantage of this method is that information about the bulk semiconductor as well as geometry of the contacts is essential.

II-8 MULTI CONTACT METHOD.

This method employs a series of identical ohmic contacts that are manufactured on the semiconductor with fixed distances between them as in Fig. 14.

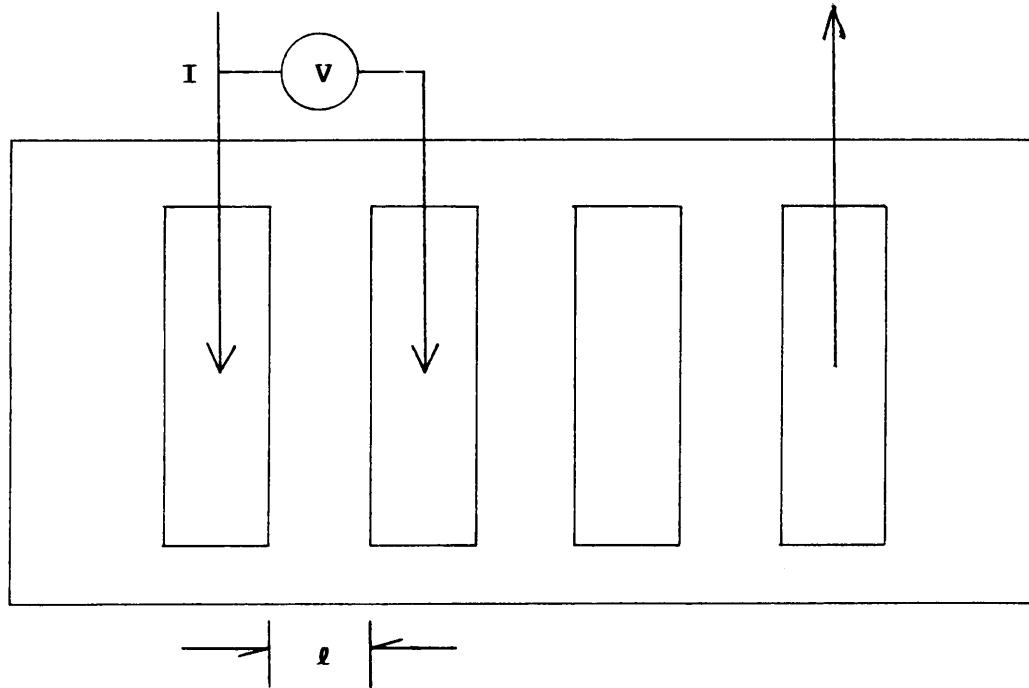


Fig 14. Series of identical ohmic contacts with spacing ℓ between them.

The total resistance measured between the first and each of the other ohmic contacts is plotted against the separation between them and is given by

$$R_t = 2R_c + R_b \quad \dots\dots\dots(\text{II-801})$$

where R_b is the resistance of the bulk semiconductor between the contacts separated by distance ℓ . Extrapolating to zero separation where $R_b = 0$ the y-intercept yields $2R_c$. From this the specific contact resistance r_c can be

determined by [10]

$$r_c = \frac{\text{y-intercept} \times A}{2} \dots\dots\dots(\text{II-802})$$

where A is the area of the ohmic contacts.

The accuracy of this method depends upon the area, the minimum distance between contacts and the number of contacts that are manufactured. Using the criteria as in II-2 we can obtain an accurate value for r_c if

$$2R_c \approx R_b \dots\dots\dots(\text{II-803})$$

From this a lower and upper value of r_c can be obtained as

$$r_{c_{\text{lower}}} = \frac{\rho l_{\text{max}} W}{20d} \dots\dots\dots(\text{II-804})$$

and

$$r_{c_{\text{upper}}} = \frac{5\rho l_{\text{min}} W}{d} \dots\dots\dots(\text{II-805})$$

where l_{max} is determined by the number of contacts used for the measurements, and l_{min} the distance between the ohmic contacts.

$$l_{\text{max}} = l_{\text{min}} \times \text{number of readings}$$

Using the test data as in II-2 and taking 6 readings when the separation

$\ell_{\min} = 1 \text{ mm}$ we find

$$r_{c_{\text{lower}}} = 2.1 \Omega.\text{cm}^2$$

and

$$r_{c_{\text{upper}}} = 35.3 \Omega.\text{cm}^2$$

To use this method the only information needed is the area of the contacts.

II-9 COMPARISON BETWEEN THE METHODS

The methods explained in the previous sections are compared by considering the following differences between them;

- (a) information required about the bulk or geometry
- (b) method of ohmic contact manufacturing
- (c) accuracy range
- (d) comments.

This is summarized in table 1, where (ρ) is the bulk resistivity, (d) the thickness of the semiconductor, (A) the area, (a) the radius of the ohmic contact and (ℓ) the spacing between two ohmic contacts.

From table 1 we observe that the simple method, the method of Jaeger and Seipp and the multi contact method are not recommended for the measurement of specific contact resistance. The simple method and the multi contact method do not include the spreading resistance term and are therefore

METHOD	INFOR- MATION	FABRICATION METHOD	ACCURACY RANGE ($\Omega.cm^2$)	COMMENTS
Simple II-2	ρ, d, A	Whole surface covered	2.0×10^{-2} 2.0	The spreading resistance not taken into account.
Spreading resis- tance II-3	ρ, d, a	Mechanical mask or lithography	1.1×10^{-2} 1.1	Accurate for fairly good ohmic contacts
Jaeger and Seipp II-4	ρ, a	Mechanical mask or lithography	1.3×10^{-2} 1.3	Approximation used is not applicable to the current flow pattern.
Anthony et. al. II-5	A	Mechanical mask or lithography	4.0×10^{-3} 8.8	Upper limit is very much limited by the area.
Transmission line II-6	None	Mechanical mask or lithography	6.3×10^{-5} 1.0×10^{-2}	The upper limit is very much determined by the input impedance of the voltmeter.
Proposed II-7	ρ, d, a, ℓ	Mechanical mask or lithography	1.0×10^{-1} 10.3	Good method for poor ohmic contacts.
Multi contact method II-8	A	Mechanical mask or lithography	2.1 35.3	Do not take spreading resistance into account

Table 1. Comparison of the different methods to determine the specific contact resistance for CdTe with a bulk resistivity of $10 \Omega.cm$.

not accurate at all. The method of Jaeger and Seipp makes an approximation to the spreading resistance for radial current flow but planar current flow is present and they do not include the bulk resistance between the two contacts in their calculation of r_c .

In conclusion, for the determination of low values for the specific contact resistance the spreading resistance (Cox & Strack), Anthony et. al and transmission line methods are recommended. When moderate to poor ohmic contacts are characterized the proposed method is recommended.

Note that the authors in table 1 did not do any calculation of ranges for which the method they used are accurate.

The value for the specific contact resistance r_c can be estimated when the bulk resistivity of the material is known, as explained on page 10. After this estimation is made it will be possible to decide which method will be used to determine r_c . For other materials like Si and GaAs, from the doping level a value for the bulk resistivity and the specific contact resistance can be estimated from graphs of bulk resistivity versus doping level and contact resistivity versus doping level. From these estimated values it can be decided which method should be used to determine r_c .

CHAPTER III METALS SYSTEMS ONTO CdTe

In this chapter the different metals and methods used to manufacture ohmic contacts to CdTe will be discussed and a summarizing table will be used. In the first part of this chapter n-type CdTe and the second part p-type CdTe will be discussed. Since no simple conversion between doping concentration and bulk resistivity exists for CdTe the bulk characteristics are given as bulk resistivity or doping concentration in the summary [1].

III-1 METAL SYSTEMS ONTO n-TYPE CdTe

From table 2 it is clear that the sample preparation, metal used for the fabrication of the ohmic contact and the annealing of the contact will determine the quality of the ohmic contact.

The formation of an ohmic contact is achieved by choosing a metal with an appropriate work-function. From the references quoted in table 2 it became clear that indium(In) is the most appropriate metal to use. This is to be expected since In has the smallest work function of those metals listed in table 2 [1].

The method used to prepare the CdTe sample will determine the quality of the ohmic contact. The best manufacturing method must therefore be found. It has been observed that for p-type CdTe, by using a dichromate etch the specific contact resistance is approximately ten times smaller than when using a bromine methanol etch [8]. This seems to be the most suitable cleaning method for CdTe, since the oxygen concentration after etching is lower with

Bulk resistivity Doping	Preparation	Metal	Fabrication	Annealing	Method used to measure r_c	Workers
10^{16} cm^{-3}	polished, etched 2% Br:methanol	In	evaporated 5×10^{-7} torr	H_2 , 300°C Cd, 900°C	Anthony et al. $10^{-3} \Omega.\text{cm}^2$	Nazaki et al[36]
—	polished, etched 5% Br:methanol	In	evaporated 10^{-6} torr	150°C to 250°C	Simple under vacuum	Braithwaite et al. [38]
—	—	In	alloying pellets at 550°C	550°C in inert gas	ohmic I–V	De Nobel [39]
10^{16} cm^{-3}	cleaved and etched	In Mn V Cr Al Ag Zn	evaporated	—	Ohmic I–V	Forsyth et al. [40]
$0.1 \Omega.\text{cm}$	Cleaved, polished etched and sputter etched	In	alloying $200^\circ\text{--}300^\circ\text{C}$	$200^\circ\text{--}300^\circ\text{C}$ for 1 hour	1.4×10^{-2} $\Omega.\text{cm}^2$	Ponpon [1]

Table 2. Comparison of the different metal systems onto n-type CdTe with the preparation methods and the methods used to evaluate the ohmic contacts.

the dichromate etch than the Br:methanol etch [8].

From table 2 the effect of annealing the ohmic contacts in an inert atmosphere is not clear, and reports on this topic are very contradictory [36,37]. The annealing process will not only decrease the specific contact resistance but change the bulk resistivity as well. Thus the bulk properties of the material are changed by annealing.

III-2 METAL SYSTEMS ONTO p-TYPE CdTe

The formation of an ohmic contact onto p-type CdTe is complicated by the fact that it is very difficult to dope the semiconductor heavily under the contact [2]. From the references quoted in table 3 it was concluded that the best result may be obtained by co-evaporation of Cu and Au on p-type CdTe. Again it is noted from Anthony et al.[8] that although the bromine: methanol etch leaves the surface more stoichiometric than the dichromate etch, the specific contact resistance is approximately ten times lower when using the latter, because of the lower oxygen concentration after etching.

Further it is observed that Au and Cu have fairly high work functions and in addition Cu acts as a p-type dopant so as to decrease the width of the potential barrier and enhance quantum mechanical current.

Bulk resistivity Doping	Preparation	Metal	Fabrication	Annealing	Method used to measure r_c	Workers
—	—	Ag Au Pt	electrolysis	—	—	De Nobel [39]
—	polished to 0.25 μm	Au	electrolysis	—	—	Mancini et al. [41]
50 $\Omega\cdot\text{cm}$	—	Au Cd_3P_2	evaporate 10^{-6} torr	pulsed laser 1W for 1ms	multi contact 0.5 $\Omega\cdot\text{cm}^2$ Au 0.15 $\Omega\cdot\text{cm}^2$ Cd_3P_2	Tews and An [10]
—	polished and etched(dichromate)	Cu/Au	evaporated	—	Anthony et al.	Fahrenbruch [2]
300 $\Omega\cdot\text{cm}$	polished or etched 10% bromine: methanol	Au	electrolysis	—	I-V character	Musa et al. [42]
3×10^{14} – 3×10^{17} cm^{-3}	polished etched $\text{K}_2\text{Cr}_2\text{O}_7$: $\text{HNO}_3:\text{H}_2\text{O}=4\text{g}:10\text{cm}^3$: 20cm^3	Au Pt	evaporated 10^{-6} torr	$200^\circ\text{--}250^\circ\text{C}$ 3 min H_2	I-V character	Gu et al. [43]

Table 3 continued next page

10^{16} cm^{-3}	polished and etched	Cr	–	–	I–V character	Williams et al. [44]
10^3 and $10^6 \text{ } \Omega\text{.cm}$	–	Cu	electrolysis	–	–	Ponpon et al. [45]
10^{15} cm^{-3}	–	Cu/Au	electrolysis	–	–	Chu et al. [46]
–	etched(dichromate)	Au	evaporated	–	–	Basol et al. [47]
0.4–1000 $\Omega\text{.cm}$	etched(dichromate)	Ni/Au	electrolysis	–	Jaeger $0.07 \text{ } \Omega\text{.cm}^2$	Jaeger and Seipp [7]
0.5 $\Omega\text{.cm}$	polished and etched(dichromate)	Cu/Au	evaporated 10^{-6} torr	–	Anthony et al. 0.1 – $0.5 \text{ } \Omega\text{.cm}^2$	Anthony et al. [8]

Table 3. Comparison of the different metal systems onto p-type CdTe with the preparation methods and the methods used to evaluate the ohmic contacts.

CHAPTER IV EXPERIMENTAL PROCEDURE

IV-I SAMPLE PREPARATION

As cut samples, 700–800 μm thick, were polished with different grid sized alumina abrasive, removing different thickness layers of CdTe, as indicated below;

5 μm alumina to remove a layer of 75 μm

3 μm alumina to remove a layer of 45 μm

1 μm alumina to remove a layer of 30 μm

0.3 μm alumina to remove a layer of 15 μm

0.05 μm alumina to remove a layer of 15 μm

After removing it from the polish block the sample was cleaned in hot tri-chloro ethylene (TCE), acetone and methanol successively and finally rinsed in deionized water . It was chemically etched by immersing the sample into a solution consisting of 7 parts saturated $\text{K}_2\text{Cr}_2\text{O}_7$: 3 parts conc. H_2SO_4 (this solution is commonly referred to as the dichromate etch) for 2 minutes. The etch was washed off by a stream of deionized water and then dried in N_2 before mounting it under a mechanical shadow mask and placing it in the vacuum system.

IV-2 CONTACT FABRICATION

The vacuum system was pumped down to 2×10^{-6} mbar before the metals were evaporated onto the semiconductor from an aluminum oxide crucible in the case when Cu/Au was used and cermit boat when In was used. The

following evaporation procedure was employed using a INFICON thickness monitor as a controller;

rise time 1	3 min
power 1	40%
idle time 1	2 min
rise time 2	2 min
power 2	50%
idle time 2	10 sec
rate	2 Å/s
density	17.8 g/cm ³
Z-ratio	0.400
tooling factor	262%
final thickness	2000 Å

The Cu and Au were co-evaporated, Cu comprising 12 at % of the evaporant. Copper and gold have similar vapor pressures and melting points and are soluble in one another at temperatures above 410°C [48]. These factors ensure the formation of a Cu/Au alloy upon evaporation from the same crucible.

When indium(In) ohmic contacts were manufactured onto n-type CdTe the same procedure was used only the density changed to 7.3 g.cm⁻³.

The sample was left in vacuum for two hours to cool down before removing and placing it in the probe station for characterization.

IV-3 METHOD FOR MEASURING r_c

After removing the samples from the vacuum system they were placed in the probe station and a graph of current through the contacts against potential difference across them was obtained for each set of ohmic contacts having the same area. From the gradient of this graph the total resistance R_t for each set of contacts was obtained. Since the currents measured are expected to be of the order of 1×10^{-6} A, all measurements were made in darkness to prevent any light induced currents.

As explained in paragraph II-7 the "proposed method" is the best suited to characterize ohmic contacts on CdTe. The proposed method (II-7) was therefore used to determine the specific contact resistance for each set of ohmic contacts. The expected values for a good ohmic contact on CdTe is not much smaller than 0.1ρ . This value for the specific contact resistance r_c favors the use of the proposed method.

The accuracy range for measuring r_c was determined for each set of ohmic contacts and if the measured value of r_c was not within this range, the value was discarded. All readings within the range were then used to determine an average value for the specific contact resistance r_c as outlined in paragraph II-7.

IV-4 AUGER ELECTRON SPECTROSCOPY

To study the cleaned semiconductor surface as explained in paragraph I-5-1 and the asymptotic overlayer discussed in I-5-4 it was decided to use Auger

electron spectroscopy because of its surface sensitivity[49].

The Auger process is based on the principle that inner shell vacancies are formed by energetic electron irradiation. The excited atoms release their energy in non-radiative transitions with the emission of electrons. The composition is then determined by measuring the energy distribution of electrons emitted during irradiation with a beam of energetic electrons. With Auger electron spectroscopy, the energy of the emergent electron is determined by the differences in binding energies associated with the de-excitation of an atom as it rearranges its electron shells and emits the Auger electrons with characteristic energies.

Fig. 15 schematically illustrates an experimental Auger apparatus placed in a high vacuum system. The cylindrical mirror analyzer has an internal electron gun whose beam is focused to a point on the sample at the source point of the cylindrical mirror analyzer. Electrons ejected from the sample pass through an aperture and are then directed through the exit aperture on the cylindrical mirror analyzer to the electron multiplier.

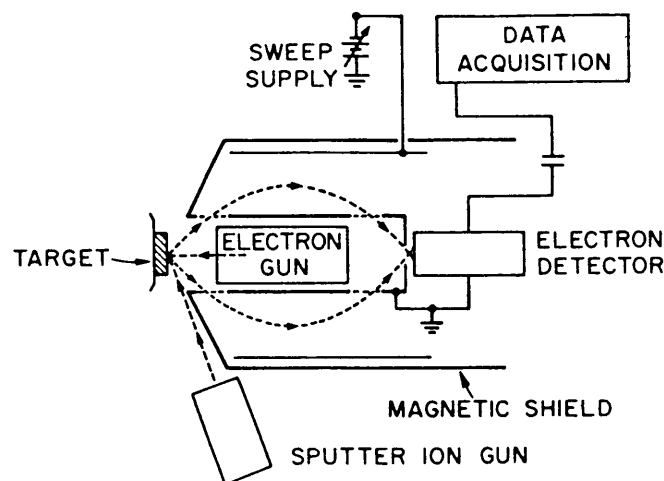


Fig. 15 Experimental apparatus used in Auger electron spectroscopy[49].

The pass energy E is proportional to the potential applied to the outer cylinder, and the range ΔE of transmitted electrons is determined by the resolution $R = \frac{\Delta E}{E}$, where R is typically 0.2 – 0.5 %. The lower value for the detection limit for impurities in the sample is 1000 ppm, \cong 0.1 atomic % [49].

With Auger electron spectroscopy the observation depth is about 3 – 20 Å and is determined by the escape depth, which is defined as the distance that electrons of well-defined energy, E_c , can travel without losing energy [49].

A major use of Auger electron spectroscopy is determining the composition as a function of depth in thin films and layered structures. The Auger signal is generated in the near surface region of the sample and ion sputtering provides the layer sectioning technique required for depth analysis. The depth profiles are shown as Auger signal height versus sputter time. Further calibrations are required to convert sputter time to depth and signal height to atomic

concentration.

As compared to other techniques such as Rutherford backscattering spectrometry, Auger depth profiling provides better depth resolution and is sensitive to both heavy and light elements. The major advantage of Auger electron spectroscopy is its sensitivity to low mass impurities, such as carbon and oxygen, which are common contaminants at surfaces and interfaces.

In order to support the electrical characterization of the ohmic contacts, limited access was obtained to the Auger system at the Physics Department of the University of Pretoria. To obtain the best advantage of the time on the system, it was decided to analyze a freshly etched CdTe surface, an In ohmic contact onto n-type CdTe and a Cu/Au ohmic contact onto p-type CdTe. All the surfaces were prepared by etching in dichromate.

IV-5 STANDARD ERROR CALCULATIONS

The standard error in the measurement of r_c will be indicated for each measurement made in chapter VI. The \pm error indicated in each of the tables in chapter VI will be that of the standard error.

The standard error will be calculated according to the following;
given that $A = xy/z$ then the standard error ΔA in A is given by,

$$\frac{\Delta A}{A} = \frac{\Delta x}{x} + \frac{\Delta y}{y} + \frac{\Delta z}{z}$$

CHAPTER V APPARATUS

V-1 VACUUM SYSTEM

The vacuum system used for evaporating the metals onto the CdTe samples was a UNIVEX 300 manufactured by Leybold Heraeus. This system makes use of a turbo molecular vacuum pump and a INFICON XTC thickness monitor. The INFICON was used as a controller, which ensured a reproducible evaporation procedure.

V-2 PROBE STATION

The SIGNATONE H-120 probe station with S-725A micro positioners and SA-T probes were used to connect the contacts in the testing circuit (Fig. 16).

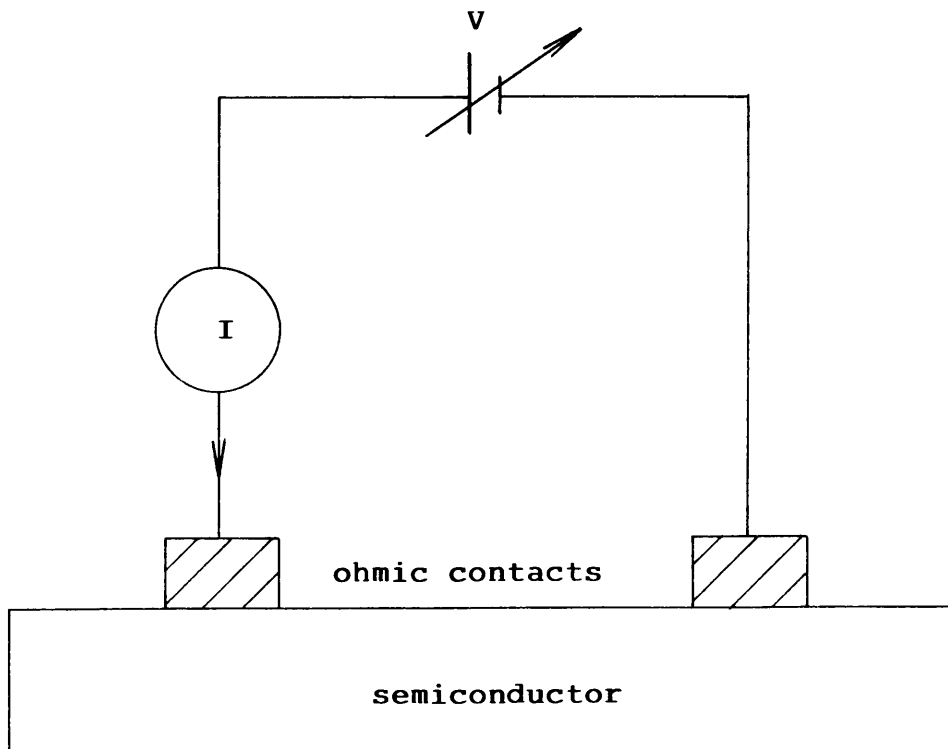


Fig. 16. The circuit diagram for the circuit used in the measurements.

V-3 CURRENT AND VOLTAGE

The HP 4140B pico Ammeter/ DC voltage source was used to supply a current through the two contacts. The potential difference was measured across the output terminals of the voltage source. The measured voltages were in the range from -10V to 10V and the current from $-1 \times 10^{-3}\text{A}$ to $1 \times 10^{-3}\text{A}$. The accuracy of the apparatus in these ranges were $\pm 0.07\% + 11\text{mV}$ for the voltage measurements and $\pm 0.5\%$ for the current measurements.

V-4 COMPUTER

The HP Integral Personal Computer was used to automate the accumulation of data and to obtain graphs of current versus voltage and perform all necessary calculations.

The HP 7475A Plotter was used to obtain a hard copy of the graph and the final results.

CHAPTER VI RESULTS AND DISCUSSION

In this chapter results and discussions will be presented for ohmic contacts on n-type and p-type CdTe. The chapter will be divided into three parts; the first will deal with ohmic contacts on n-type CdTe while the second will deal with p-type CdTe. The third part of this chapter will deal with observations on surface preparation before manufacturing the ohmic contacts, the proposed method for determining r_c and a design procedure for a mechanical mask.

PART I OHMIC CONTACTS TO n-TYPE CdTe

VI-1 SAMPLE 1

The aim with this sample was to do a trial run with indium(In) onto n-type CdTe and investigate if a measurable current could be passed between two ohmic contacts on either side of a CdTe sample.

The sample was a n-type Cl doped CdTe sample of unknown resistivity obtained from the CSIR in South Africa. The sample was prepared as explained in IV-1 and then etched in a solution of 2% bromine and methanol for 5 minutes.

Two indium(In) ohmic contacts were evaporated in a vacuum of 1×10^{-5} mbar onto the CdTe, one on the front with a diameter of 1mm and the other on the back with a diameter of 2mm.

The ohmic contacts were then characterized by placing the sample in the

probe station and the graph of current versus voltage were obtained. From Fig. 17 we observe that a measurable current is flowing through the contacts but that the contacts are not ohmic.

The average value for the total resistance between the two contacts as calculated from Fig. 17, between voltages of -0.7V and 0.7V , will not be accurate because of the diode-like behavior of the contacts. Nevertheless a value for the total resistance $R_t = 10^7 \Omega$ was obtained that gives an indication of the order of magnitude for the total resistance between the two contacts.

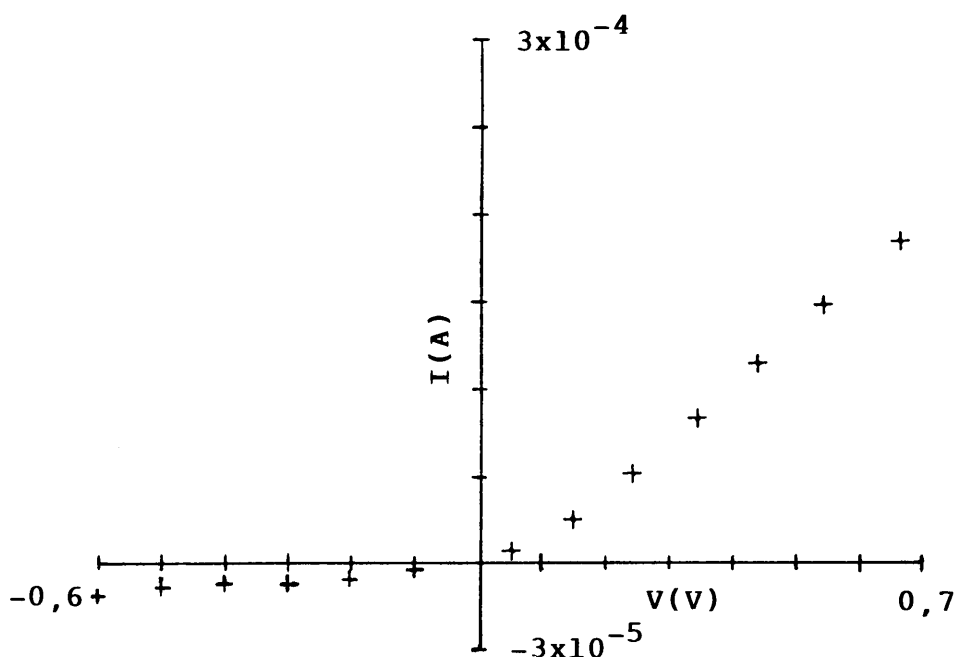


Fig. 17. The graph of current against voltage for In ohmic contacts on n-type Cl-doped CdTe (sample 1).

The diode-like behavior of the contacts can be explained by the fact that In on n-type CdTe forms a barrier with a height of 0.5 eV [1]. When the doping beneath the contact is low or a suitable interface is not formed the barrier will

be wide and thermionic emission rather than tunneling will be the dominant current transport mechanism. This yields a diode like behavior instead of an ohmic.

VI-2 SAMPLE 2

This sample was a Cl doped n-type CdTe sample from the same ingot as sample 1 with a bulk resistivity of $1.41 \times 10^{-1} \Omega \cdot \text{cm}$ as determined using Van der Pauw measurements at 300 K by the CSIR.

The In ohmic contacts were manufactured as explained in IV-1 and IV-2 and were approximately 2000 \AA thick. The contact configuration used is shown in Fig. 18. The final thickness of the CdTe after polishing and etching was $365 \mu\text{m}$ as measured with a metallurgical microscope.

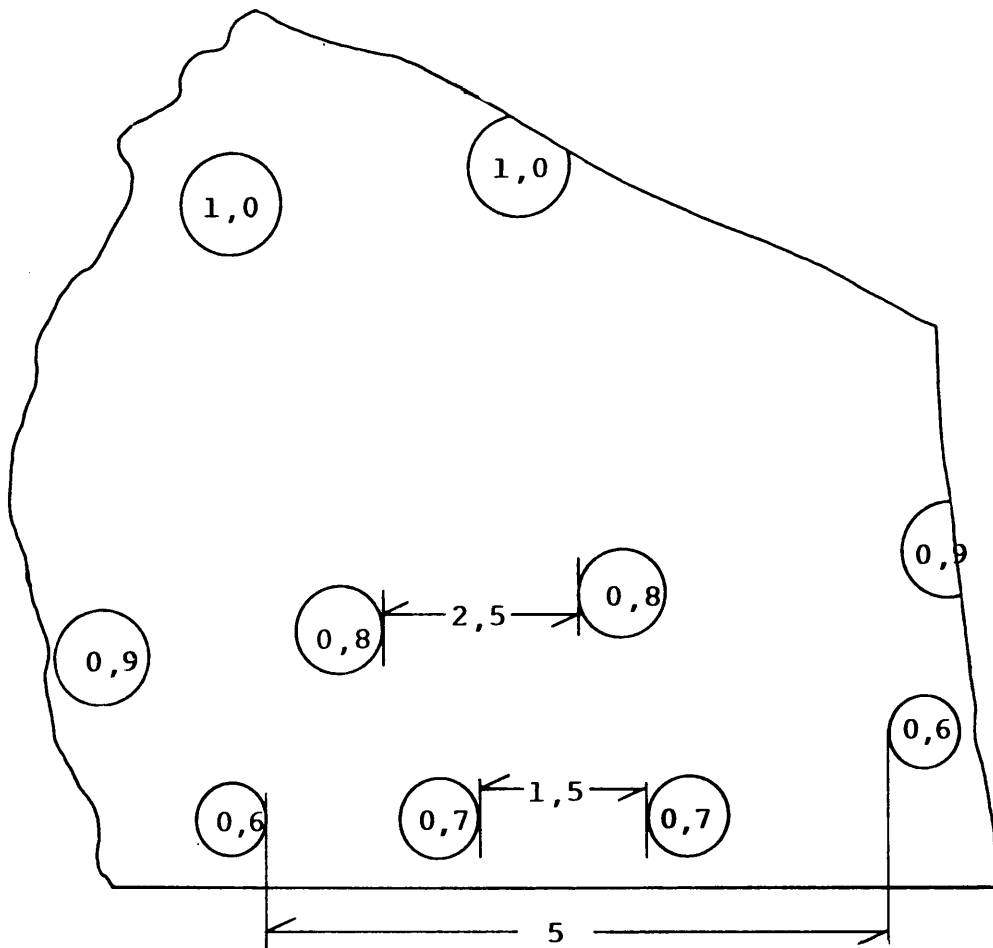


Fig. 18. The contact configuration obtained with the use of a mechanical mask on sample 2.

The sample was then characterized by placing it in the probe station and obtaining the graph of current versus voltage for each set of ohmic contacts having the same diameter, from these it was deduced that all the contacts were ohmic. The total resistance R_t was calculated from these graphs and the specific contact resistance r_c was calculated using equation II-707. The results are tabulated in table 4. The specific contact resistance values for the 0.9 mm and 1.0 mm diameter contacts were not calculated since they were not properly formed on the CdTe sample. The proposed method used requires two identical contacts for the calculations. For all the other sets of contacts the specific contact resistances calculated were within their accuracy range and were used to calculate an average value of r_c for the sample.

Diameter (cm) $\times 10^{-1}$	Spacing (cm) $\times 10^{-1}$	R_t (Ω)	r_c ($\Omega \cdot \text{cm}^2$) $\times 10^{-1}$	Accuracy range ($\Omega \cdot \text{cm}^2$)
0.6	5.00	174	1.8	6.2×10^{-3} – 6.2×10^{-1}
0.7	1.50	136	2.3	3.1×10^{-3} – 3.1×10^{-1}
0.8	2.50	110	2.3	4.9×10^{-3} – 4.9×10^{-1}
Average r_c			$2.1 \pm 1.15 \times 10^{-2} \Omega \cdot \text{cm}^2$	

Table 4. The results obtained for sample 2, In ohmic contacts on a Cl doped n-type CdTe of thickness $365 \mu\text{m}$ and bulk resistivity $1.41 \times 10^{-1} \Omega \cdot \text{cm}$.

According to the classification on page 10 and compared to the results of Ponpon[1] the contacts manufactured here are poor. The quality of the ohmic contacts can possibly be improved by investigating different cleaning and evaporation procedures. However, when the sample is annealed at temperatures higher than 100°C it is predicted[5], that the bulk resistivity will change because of In diffusion into the CdTe and changing the doping concentrations. Thus annealing the sample in order to improve the quality of the contacts is not recommended.

To investigate the In/CdTe interface prepared by a dichromate etch, Auger spectroscopy was performed on the sample (Fig. 19). This revealed that the In diffused into the CdTe and most probably chemically binds to the excess tellurium (Te) that was produced by the chromate etch. Indium and Te do form a stable compound in the form of In_2Te_3 [50] and InTe [49]. The oxygen throughout the In layer into the CdTe might be attributed to the fact that the

sample was exposed to the atmosphere for 3 months before being able to do the Auger electron spectroscopy. Similar work has been done on p-type CdTe using Auger electron spectroscopy[8] and Rutherford backscattering[41]. Alternatively oxygen might have been present even before or during evaporation of the In.

It was also evident from Fig. 19 that the oxygen throughout the In layer into the CdTe could be the cause for not obtaining a very good ohmic contact.

Samples 1 and 2 were cut from the same ingot. Their positions relative to each other in the ingot was not known and it was therefore not possible to assume the same bulk resistivity for the two samples. The size of sample 1 was so small that Van der Pauw measurements could not be carried out to determine its bulk resistivity. In order to compare sample 1 and 2 it is observed that the total resistance between the contacts is much larger for sample 1 than for sample 2. If it is assumed that the bulk resistivity of the two samples are close to the same value then this indicates that the sample prepared using the dichromate etch results in a much lower total resistance as for a sample prepared using the Br:methanol etch. These findings are supported by Anthony et al. [8].

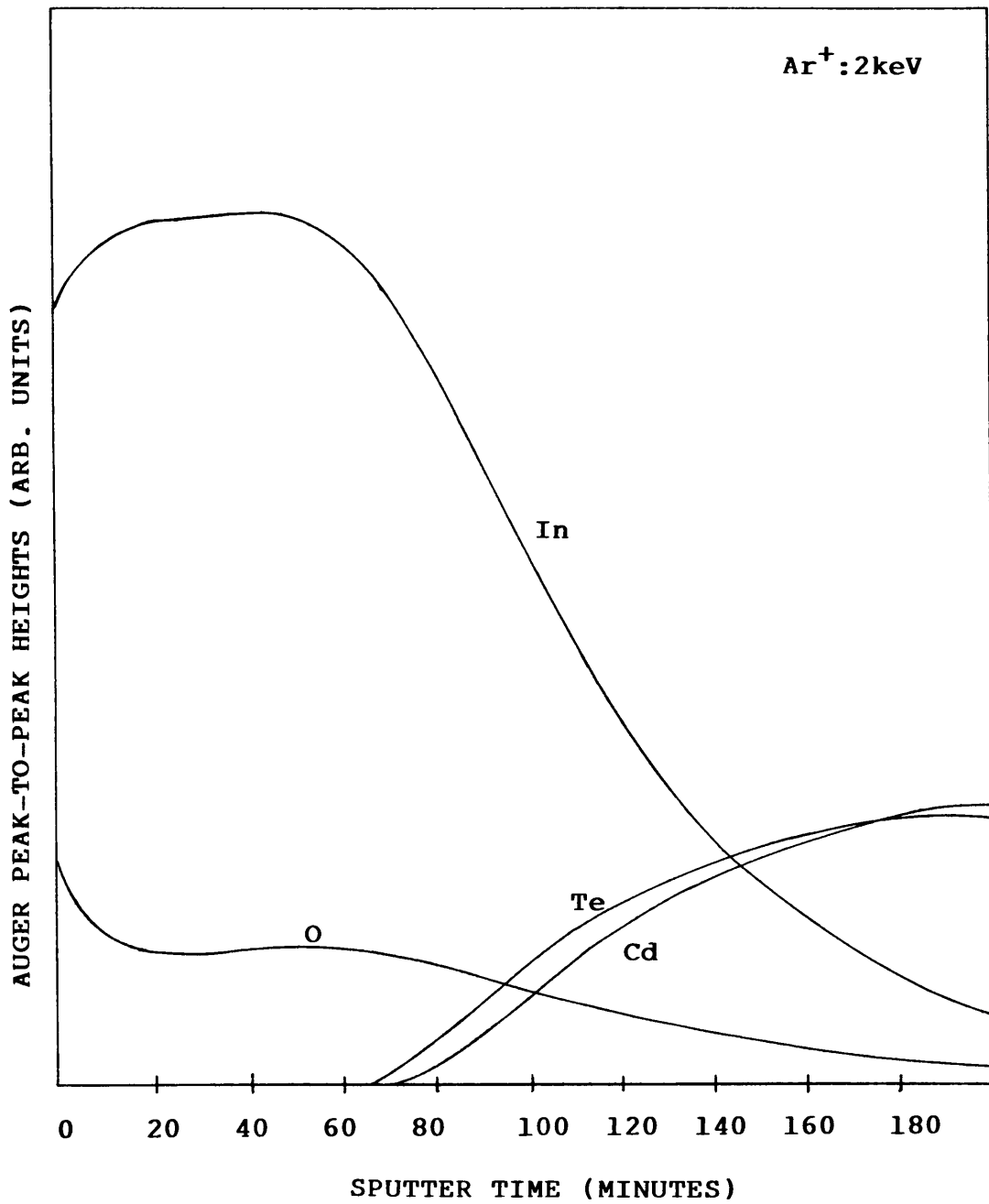


Fig. 19. Sputter profile obtained from the Auger peak to peak values (in arbitrary units) for an In layer on n-type CdTe which was etched with dichromate.

VI-3 SAMPLE 3

This sample was slice 22 of 27, Cl-doped n-type CdTe, grown by the CSIR and an estimated bulk resistivity of $\approx 10^3 \Omega \cdot \text{cm}$ was supplied.

The sample preparation and contact manufacturing are done as explained in IV-1 and IV-2. The thickness of the In contacts were 3000 \AA and the thickness of the CdTe sample $635 \mu\text{m}$. The mechanical mask that was used resulted in a contact configuration as in Fig. 20.

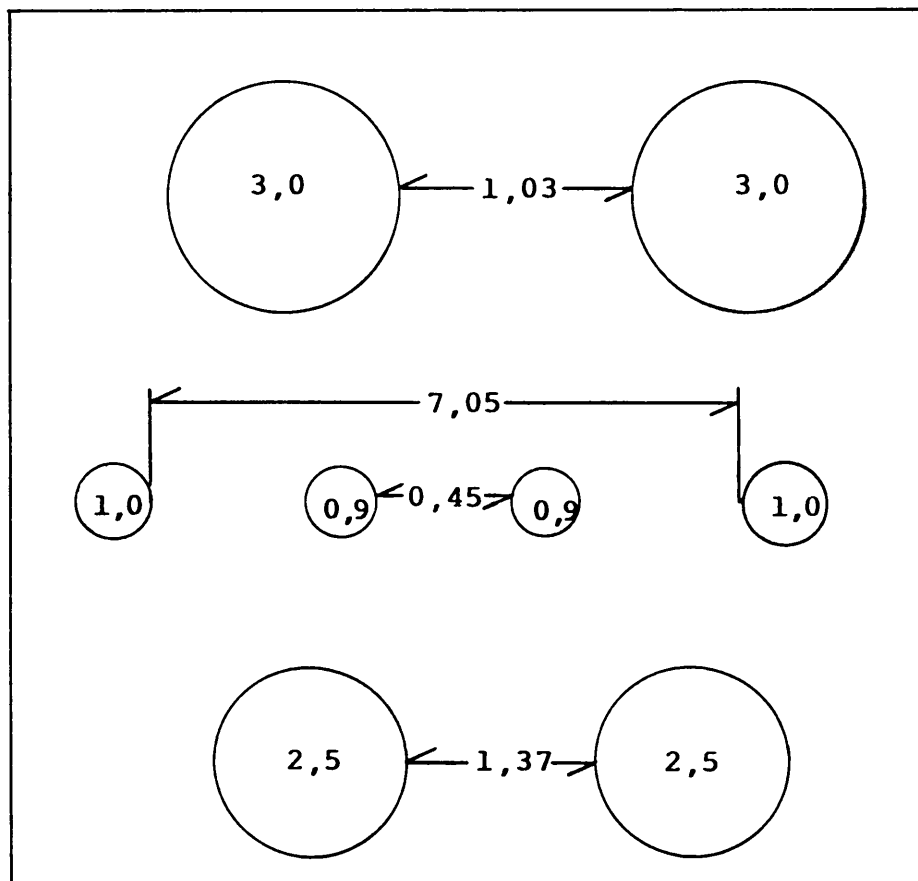


Fig. 20. The mechanical mask used with sample 3 produced the above contact configuration.

A standard mask had not yet developed and this experimental mask was utilized.

From the graphs of current versus voltage for the different sets of contacts it was observed that the contacts were ohmic and the values of R_t were calculated, but since no accurate value was available for the bulk resistivity, no accurate value could be calculated for the specific contact resistance.

Assuming the value for bulk resistivity $\rho = 4 \times 10^3 \Omega \cdot \text{cm}$, the results as in table 5 are obtained. The specific contact resistance calculated for the 0.9 mm, 2.5 mm and the 3 mm diameter contacts were all outside the range for which they could be calculated accurately and therefore r_c should not be considered as accurate. The value of r_c in table 5 is therefore that of the 1mm contact only.

Diameter (cm) $\times 10^{-1}$	Spacing (cm) $\times 10^{-1}$	R_t (Ω) $\times 10^6$	r_c ($\Omega \cdot \text{cm}^2$) $\times 10^3$	Accuracy range ($\Omega \cdot \text{cm}^2$)
0.90	0.45	6.07	18.8	48.9 – 4893
1.00	7.05	5.23	18.2	237.2 – 23721
2.50	1.37	1.98	46.8	184.7 – 18465
3.00	1.03	3.71	129.2	192.9 – 19292
r_c			$18.2 \times 10^3 \pm 2.1 \times 10^2 \Omega \cdot \text{cm}^2$	

Table 5. The results obtained for sample 3, In ohmic contacts on a Cl doped n-type CdTe of thickness 635 μm and bulk resistivity $4 \times 10^3 \Omega \cdot \text{cm}$.

The sample was cut near the end of the ingot and therefore the bulk characteristics may have been non-uniform resulting in only the 1mm contact

on an area having the same bulk characteristics.

As a test the sample was annealed in an argon atmosphere for 3 hours at a temperature of 100°C and the above measurements repeated (table 6). Unfortunately it was not possible to perform Van der Pauw measurements on the sample to check if the bulk resistance of the CdTe changed with the annealing process, and therefore no calculation of the specific contact resistance were made.

Diameter (cm) $\times 10^{-1}$	Spacing (cm) $\times 10^{-1}$	R_t (Ω)
0.90	0.45	69.872
1.00	7.05	41.376
2.50	1.37	198.697
3.00	1.03	104.128

Table 6. The values of R_t obtained for sample 3 after it was annealed in an argon atmosphere for 3 hours at a temperature of 100°C.

From the total resistance, R_t , measured on sample 3 before and after annealing in an argon atmosphere at a temperature of 100°C for 1 hour, it is clear that the contact resistance and/or the bulk resistivity changed drastically. R_t has decreased from $6.07 \times 10^6 \Omega$ to $6.987 \times 10^1 \Omega$ during the annealing process for the contact with a diameter of 0.09 cm. Since In is an n-type dopant in CdTe it is possible that it diffused into the CdTe to change the doping level and thus reduce the bulk resistivity and specific contact resistance. The fact that the bulk resistivity might have changed is supported by Giles et al. [5], and the change in specific contact resistance by Nazaki et al. [36].

PART II OHMIC CONTACTS ONTO p-TYPE CdTe

VI-4 SAMPLE 4

The aim in using this sample was to do a trial run with Cu/Au on p-type CdTe and investigate if a measurable current could be passed between two ohmic contacts. The sample had a high unknown bulk resistivity. The sample was obtained from the CSIR which in turn was obtained from a source in the U.S.A.

The procedure as outlined in IV-1 and IV-2 was used to prepare the sample and to manufacture the ohmic contacts with a thickness of approximately 2000 Å. Two contacts were manufactured on the same side of the CdTe sample so that the current was flowing from top to top of the sample.

Since the sample was very small and only two contacts could be manufactured on the sample and the bulk resistivity was not known, the specific contact resistance could not be determined using the proposed method. The ohmicity of the contact was investigated by placing the sample in the probe station and obtaining a graph of current against voltage as shown in Fig. 21.

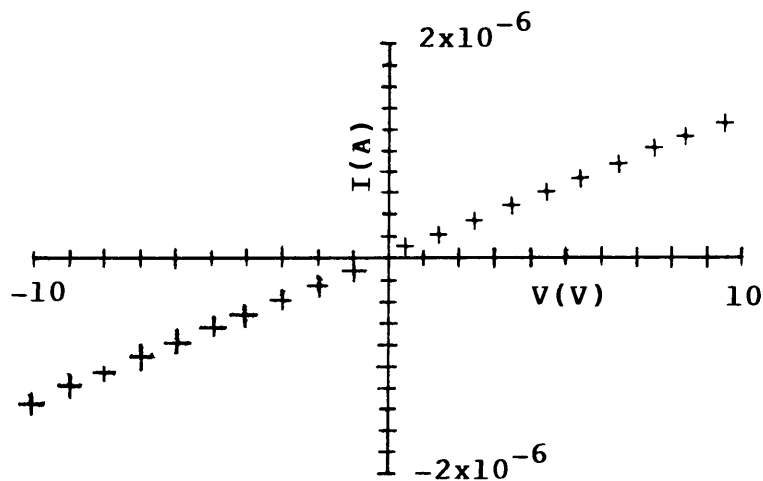


Fig. 21 The graph of current versus voltage for Cu/Au ohmic contacts on p-type CdTe (sample 2).

From this graph it is observed that Cu/Au does form an ohmic contact on p-type CdTe and a measurable current can be passed between two contacts on the same side of a CdTe sample.

VI-5 SAMPLE 5

This was a low resistivity $\approx 10^1 \Omega \cdot \text{cm}$ p-type CdTe sample obtained from MCP in the United Kingdom.

The sample was prepared as explained in IV-1 and the Cu/Au contacts manufactured as explained in IV-2.

As the sample was removed from the mechanical mask it broke into small pieces so that no measurement of specific contact resistance could be made. It

was possible to obtain a graph of current versus voltage for a set of contacts of different sizes and this showed that the contacts were indeed ohmic. The proposed method does not allow for the measurement between two contacts of different sizes.

From the measurements made between a 0.25 mm and a 0.3 mm contact using the proposed method a specific contact resistance of $30 \Omega \cdot \text{cm}^2$ was obtained on a 450 μm thick CdTe sample with a bulk resistivity of $10 \Omega \cdot \text{cm}$. The spacing between the two contacts was 1.03 mm. The diameter used in the calculations of r_c was 0.3 mm.

VI-6 SAMPLE 6 (1st)

This sample was a (100) orientated p-type CdTe obtained from II-VI in the U.S.A. The bulk resistivity as supplied, determined using the Van der Pauw method, was $175 \Omega \cdot \text{cm}$.

The sample preparation and contact manufacturing were performed as outlined in IV-1 and IV-2. The sample thickness was measured as 783 μm and the contact thickness as 2000 \AA . The mechanical mask used produced a contact configuration as shown in Fig. 22.

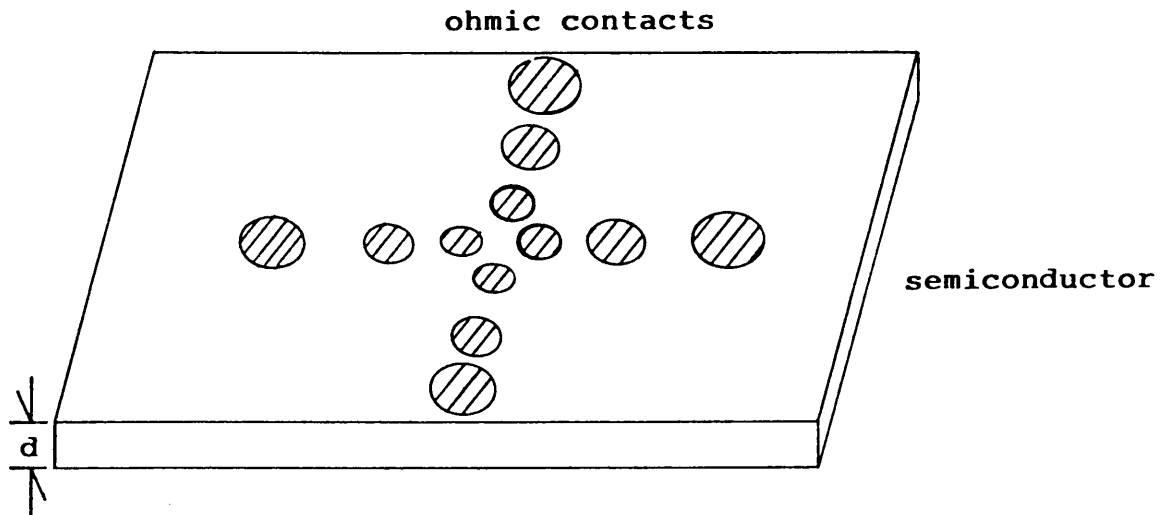


Fig. 22. The contact configuration as obtained for sample 6 (1st) using a mechanical mask.

The sample was placed in the probe station and the results obtained are given in table 7. From the graph of current versus potential for each set of contacts it was clear that the contacts were ohmic. The specific contact resistance calculated for each set of contacts were within the range for which the method is accurate and were thus used for calculating an average value for the specific contact resistance of the sample.

Diameter (cm) $\times 10^{-1}$	Spacing (cm) $\times 10^{-1}$	R_t (Ω) $\times 10^4$	r_c ($\Omega \cdot \text{cm}^2$)	Accuracy range ($\Omega \cdot \text{cm}^2$)
0.313	1.587	24.10	73.5	1.7 – 174.3
0.496	1.604	12.50	97.7	2.4 – 239.1
0.633	1.867	6.98	82.1	3.2 – 318.5
0.700	2.600	7.23	104.6	4.3 – 434.9
0.800	4.300	5.41	84.6	7.2 – 723.6
1.000	3.900	3.91	95.7	8.3 – 828.2
Average r_c			$89.7 \pm 4.2 \times 10^{-2} \Omega \cdot \text{cm}^2$	

Table 7. The results obtained for sample 6 (1st), Cu/Au ohmic contacts on (100) p-type CdTe of thickness 783 μm and bulk resistivity of 175 $\Omega \cdot \text{cm}$.

The quality of the contact is moderate according the classification on page 10. The fairly high value of r_c can be attributed to the fact that it is difficult to dope CdTe directly under the contact. This reduces the quantum mechanical tunneling current flowing, because of a wider barrier. As the bulk resistivity increases the difficulty to dope the region directly beneath the ohmic contact increases drastically.

VI-7 SAMPLE 6 (2nd)

The ohmic contacts of sample 6 (1st) were removed by lapping it with 400 grid paper. Thereafter sample preparation and contact manufacture procedure as in IV-1 and IV-2 were used to manufacture a new set of Cu/Au ohmic contacts onto the p-type CdTe of 175 $\Omega \cdot \text{cm}$ of which the final thickness was 610 μm .

The mechanical mask utilized in manufacturing the ohmic contacts produced a configuration as shown in Fig. 23. The same size drills as used to manufacture the mask in Fig. 22 were used to manufacture this mask. Using this mask, two sets of contacts ranging from 0.3 mm to 1 mm in diameter could be produced and a larger number of readings of specific contact resistance could be obtained and used to calculate an average value of r_c for the sample. The mask was poorly manufactured and the only sets of contacts that were usable are those listed in table 8.

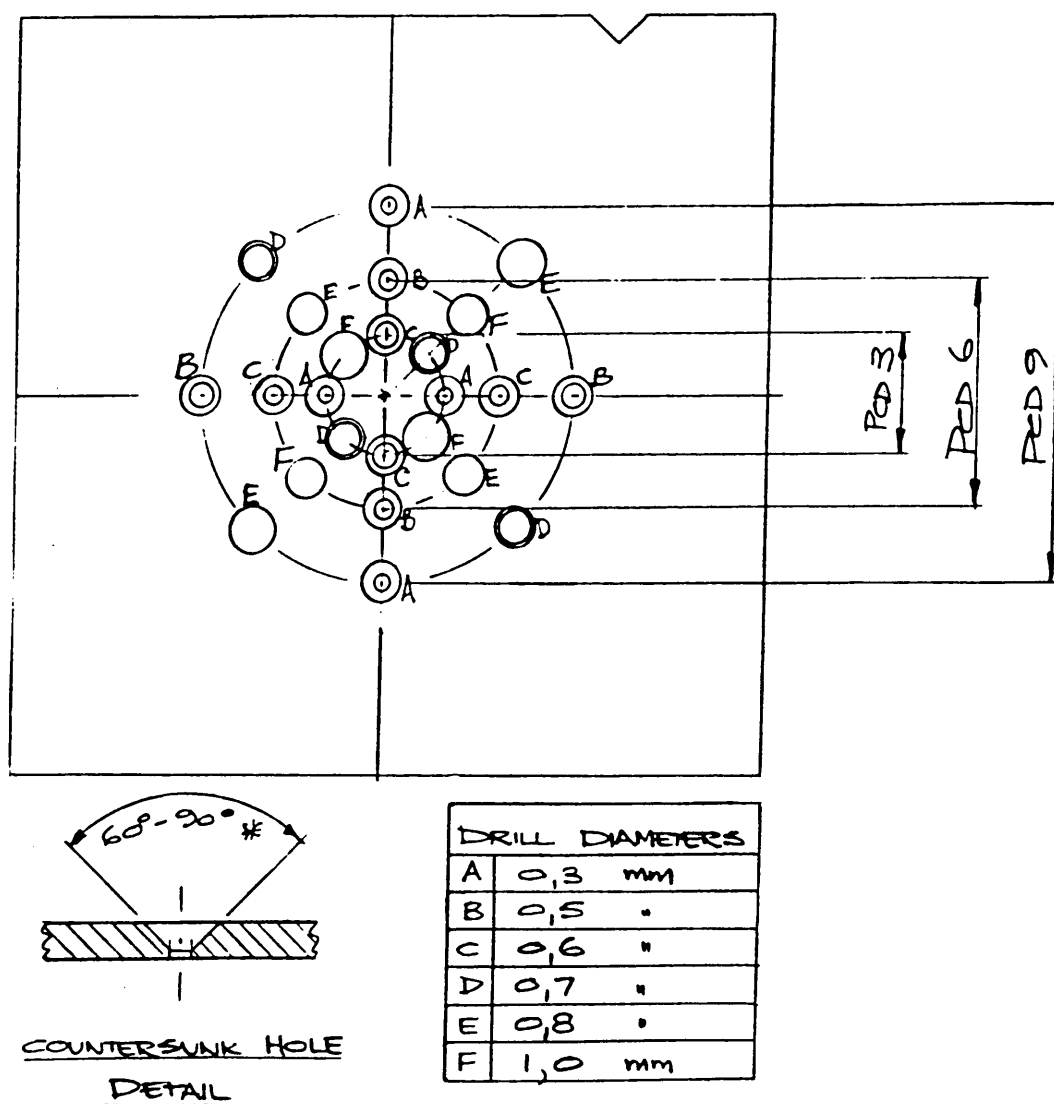


Fig. 23. The configuration of ohmic contacts produced on sample 6 (2nd).

After the sample was removed from the vacuum system and placed into the probe station, the results tabulated in table 8 were obtained. From the plot of current versus potential for each set of contacts from which the total resistance were calculated it was observed that the contacts were indeed ohmic.

Diameter (cm) $\times 10^{-1}$	Spacing (cm) $\times 10^{-1}$	R_t (Ω) $\times 10^4$	r_c ($\Omega \cdot \text{cm}^2$)	Accuracy range ($\Omega \cdot \text{cm}^2$)
0.356	2.625	16.30	57.6	2.5 – 251.8
0.595	5.929	17.20	181.0	7.2 – 715.4
0.715	2.318	10.30	171.4	4.1 – 408.9
0.756	2.007	9.17	171.8	3.9 – 389.7
0.876	5.661	8.35	171.1	9.9 – 989.4
1.073	1.946	6.30	240.0	5.3 – 528.7
Average r_c			$165.5 \pm 9.3 \times 10^{-1} \Omega \cdot \text{cm}^2$	

Table 8. The results obtained for sample 6 2nd, Cu/Au ohmic contacts on (100) p-type CdTe of thickness $610 \mu\text{m}$ and bulk resistivity of $175 \Omega \cdot \text{cm}$.

The specific contact resistance calculated for all the sets of contacts were within the range for which the method is accurate and were therefore used to obtain an average value of r_c for the sample.

The mask used was studied under a light microscope with a 200X magnification which revealed that the mask was very poorly manufactured and could not be used for routine work. The mask was 1.5 mm thick and all the holes were countersunk at an angle of $60^\circ - 90^\circ$ (as shown in Fig. 23) to a thickness of approximately $600 \mu\text{m}$. This investigation showed that in order to

obtain two identical contacts the mask must not be thicker than 300 μm . This mask was thus not used for any further work.

VI-8 SAMPLE 6 (3rd)

The ohmic contacts of sample 6 (2nd) were once again removed as described above and a new set of contacts manufactured. The final thickness of the sample was 454.5 μm .

The same mechanical mask as with sample 6 (1st) was used because, as explained in paragraph VI-8, the latest mask was not usable. The configuration of contacts as in Fig. 22 was obtained. The contacts were analyzed and the results are tabulated in table 9. From the plots of current versus potential it was clear that the contacts were ohmic.

Diameter (cm) $\times 10^{-1}$	Spacing (cm) $\times 10^{-1}$	R_t (Ω) $\times 10^5$	r_c ($\Omega \cdot \text{cm}^2$)	Accuracy range ($\Omega \cdot \text{cm}^2$)
0.313	1.587	9.12	333.4	1.7 – 174.3
0.496	1.604	4.07	369.2	2.4 – 239.1
0.633	1.867	3.44	509.4	3.2 – 318.5
0.700	2.600	2.56	449.1	4.3 – 434.9
0.800	4.300	2.50	555.9	7.2 – 723.6
1.000	3.900	2.07	730.1	8.3 – 828.2
Average r_c			643.0 \pm 3.0 $\Omega \cdot \text{cm}^2$	

Table 9. The results obtained for sample 6 (3rd), Cu/Au ohmic contacts on (100) p-type CdTe of thickness 454.5 μm and bulk resistivity of 175 $\Omega \cdot \text{cm}$.

From table 9 it can be seen that only the specific contact resistances for the 0.8 mm and the 1 mm diameter sets of contacts were within the range for which the method is accurate and were thus used to obtain an average value of r_c .

The application of the proposed method to samples 6 (1st), 6 (2nd) and 6 (3rd) illustrates that the method can be applied to a wide range of values for the specific contact resistance r_c .

The increase of specific contact resistance as the thickness of the CdTe decreases might be attributed to the fact that mechanical damage penetrates approximately 10 times deeper into CdTe than in Si or GaAs [51]. Each time sample 6 was polished from the same side when removing the contacts manufactured previously. Each time the sample was mounted on the polish block with wax by heating it to 70°C. This heating might have enhanced the migration of the sawing damage from the as cut face towards the side that was to be polished. After repeating the process 3 times it might have been possible to polish into damaged region of the semiconductor substrate. Thus with sample 6 (2nd) and 6 (3rd) ohmic contacts might have been manufactured onto degraded material which will result in poor ohmic contacts.

It is difficult to heavily dope CdTe directly beneath the ohmic contact and low doping levels decrease the electrical quality of the ohmic contact. This results in the poor formation of ohmic contacts on CdTe. Very little have been published on high bulk resistivity (low doping levels) CdTe, and the methods used to determine the specific contact resistance were in most cases unaccurate.

The possibility exist that other researchers have removed all polish damage with the chemical etch. This might not have been achieved with sample 6.

Auger spectroscopy was performed on a Cu/Au contact on a CdTe sample prepared by etching in dichromate. From the results (Fig. 24) it can be seen that the sample was contaminated with oxygen before manufacturing of the contacts. It is clear that the Cu diffused into the CdTe surface and it seems as if it is chemically bound with the excess Te produced by the chromate etch to form CuTe_2 [8].

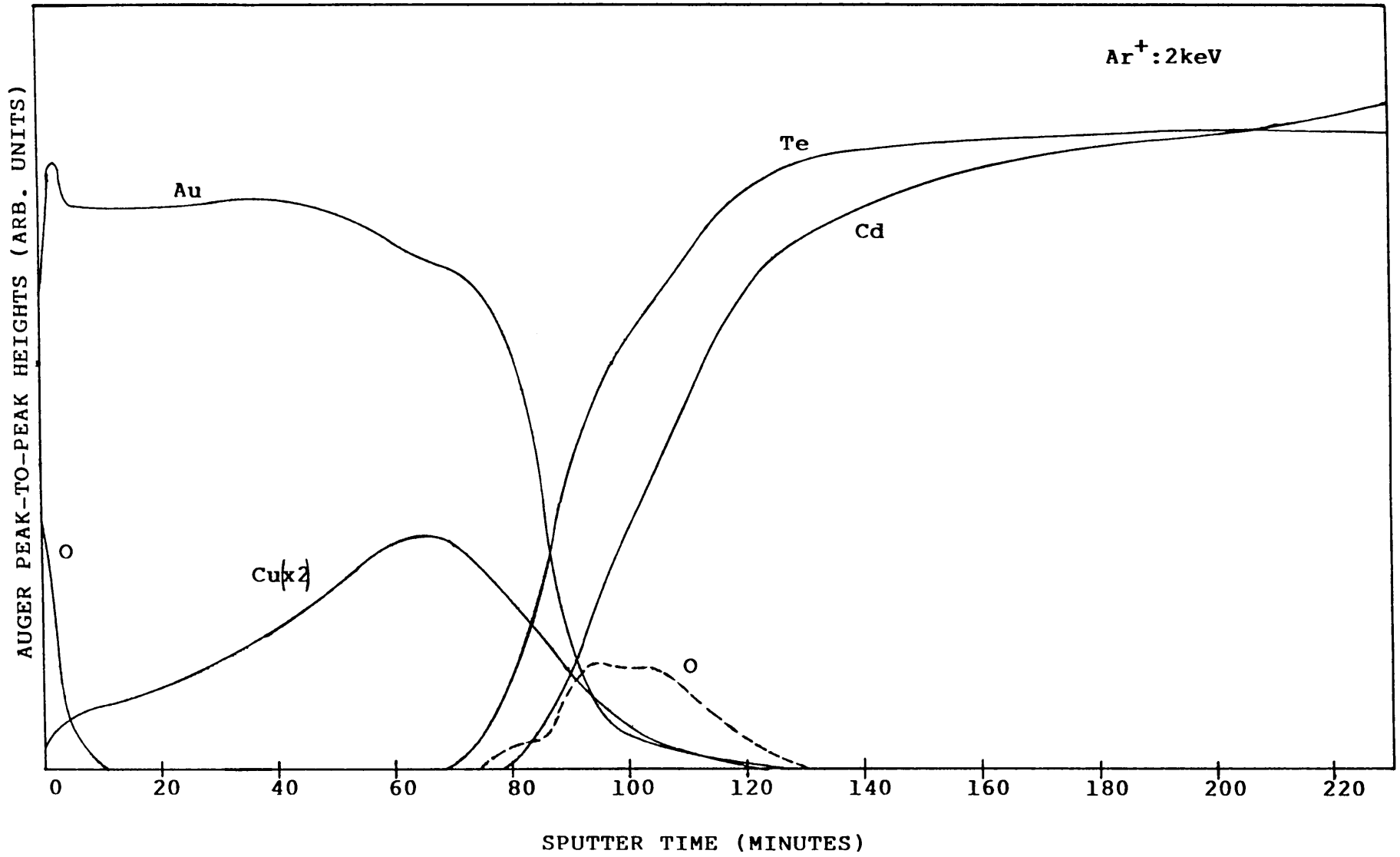


Fig 24 Auger peak to peak heights (in arbitrary units) for a Cu/Au contact onto p-type CdTe prepared by etching in dichromate.

Sample	Type	Orientation	Bulk resistivity ($\Omega.cm$)	Thickness (μm)	Metal	r_c ($\Omega.cm^2$)	Comments
1	n	—	—	—	In	—	Non-ohmic I-V; Br: methanol etch
2	n	—	1.41×10^{-1}	365	In	2.1×10^{-1}	Dichromate etch
3	n	—	$\approx 10^3$	635	In	18.2×10^3	Dichromate etch
4	p	—	—	—	Cu/Au	—	Ohmic from I-V
5	p	—	low ≈ 10	450	Cu/Au	30.0	Ohmic from I-V
6 1st	p	(100)	175	783	Cu/Au	86.7	Dichromate etch
6 2nd	p	(100)	175	610	Cu/Au	165.5	"
6 3rd	p	(100)	175	454.5	Cu/Au	643.0	"

Table 10. A summary of the results obtained for the samples that was suitable to test.

PART III OBSERVATIONS

VI-9 SUMMARY OF THE RESULTS AND DISCUSSION

The results are summarized in table 10 so that an overall view can be obtained.

From table 10 it can be seen that In on n-type CdTe does form good ohmic contacts when the dichromate etch is used. Samples prepared by etching in dichromate result in ohmic contacts of better quality than those prepared by etching in a Br:methanol etch.

For the p-type CdTe it is observed that Cu/Au does form an ohmic contact. It is also observed that the proposed method can be used to calculate the specific contact resistance of a wide range of CdTe samples of different bulk resistivities.

VI-9-1 Method for determining r_c

Many of the methods for measuring r_c make use of the approximation $2a \ll d$, where a is the radius of ohmic contacts and d the thickness of the CdTe sample. The samples used in the present experimental work had a thickness ranging between $450 \mu\text{m}$ and $800 \mu\text{m}$ and the contact diameters ranged from 0.313 mm to 3 mm . These values of a and d do not satisfy this approximation and hence these methods are not appropriate to determine r_c .

The values of the specific contact resistance measured on the samples, using

the proposed method, were all well within the ranges for which the method is accurate.

VI-9-2 Sample preparation

The large difference in the current flowing through the contacts of sample 1 and 2, with the same bulk resistivities but close to each other with different sample preparation, shows that the dichromate etch produces a better quality ohmic contact than when using a Br:methanol etch [8].

The clean semiconductor surface as discussed in I-5-1 was investigated by performing Auger electron spectroscopy on a freshly dichromate etched CdTe surface. From Fig. 25, the CdTe surface is Te rich with a fairly low oxygen concentration. Carbon and sulphur were also detected but with very low concentrations. Anthony et al. did a comparative study of a CdTe surface etched with dichromate and Br:methanol where they found the dichromate yielded a lower concentration of oxygen[4]. The Br:methanol etched ensured a more stoichiometric surface than the dichromate etch. The excess Te on the surface due to the dichromate etch seems to enhance the formation of an interfacial layer of InTe or In_2Te_3 .

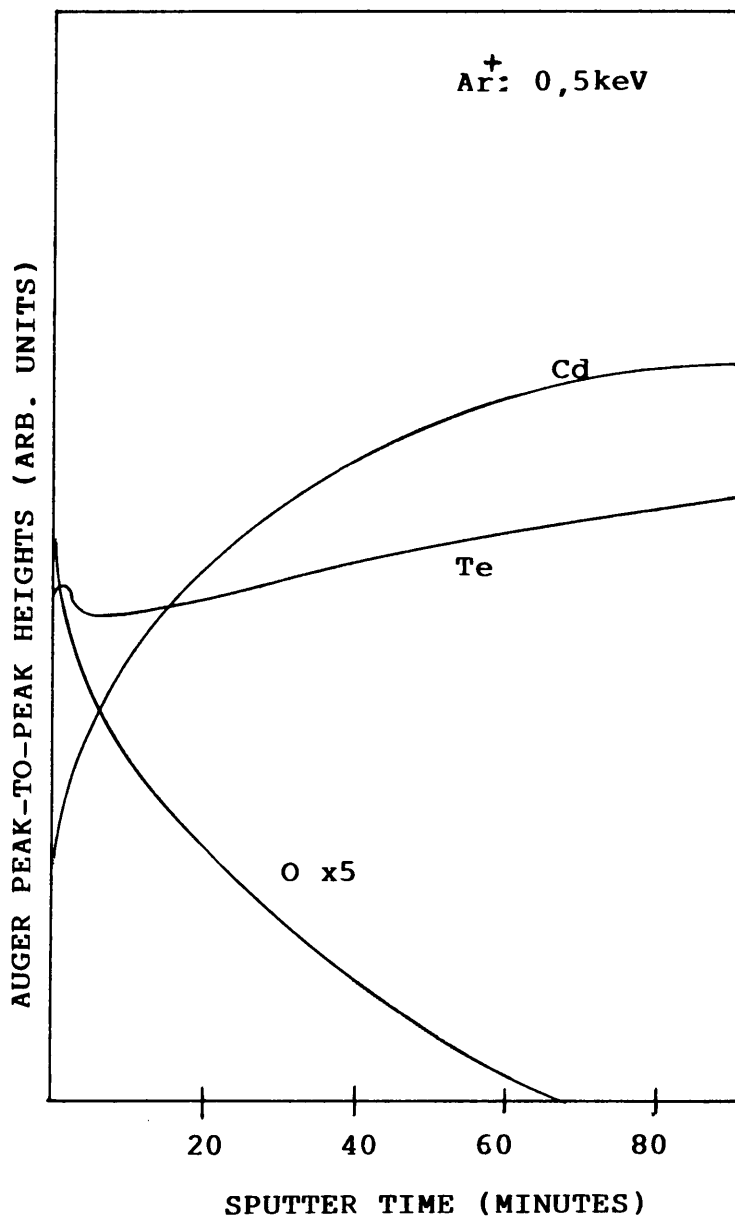


Fig. 25 Auger peak to peak heights (in arbitrary units) for a freshly dichromate etched surface of CdTe.

VI-9-3 Mechanical mask

The analysis of sample 6 (1st), 6 (2nd) and 6 (3rd) shows that a good thin mask is essential in producing sets of identical contacts. These results also

indicate that the mask used resulted in contacts having a wide range of specific contact resistance values, that can accurately be determined for a wide range of bulk resistivity CdTe.

To establish guidelines for designing a mechanical mask that will have a large range of specific contact resistances which can accurately be calculated with the proposed method for all sets of contacts, the variables that influence the range were investigated.

Since the diameter of a contact is to some extent determined by the availability of drills, the diameters were fixed to 0.313 mm, 0.496 mm, 0.633 mm, 0.700 mm, 0.800 mm and 1.000 mm. Those were the diameters for the holes in the mechanical mask used for contact manufacturing on sample 6 (1st) and 6 (3rd). The thicknesses of the samples were between 400 μm and 800 μm . The only variable that influences the accuracy of the specific contact resistance calculation is the contact separation ℓ .

In section II-7 when the upper and lower limit for the values of r_c were calculated, we used equation II-708 with the criteria used in II-2; that the one term can be ten times the other in order to measure them accurately. For

the upper limit of r_c the ratio of $\frac{2R_c}{2R_c + R_b + R_o} = 10$ and for the lower limit the ratio of $\frac{2R_s + R_b + R_o}{2R_c} = 10$. The ideal mechanical mask will have these

ratio's as close to 1 as possible. The spacing of the contacts from each other will very strongly affect these ratio's. A visual picture was obtained by drawing a graph of $\frac{2R_c}{2R_s + R_b + R_o}$ against contact separation ℓ for each set of

contacts on a sample with a given bulk resistivity. The results of sample 6 (1st), 6 (2nd) and 6 (3rd) were used to obtain Figs. 26, 27 and 28, respectively. From these figures it is observed that in order to obtain good accuracy for the specific contact resistance for all sets of contacts, small diameter contacts must be further apart than their larger counterparts, since this yields ratio's nearest to 1.

It is also observed that, as the quality of the contact decreases, the ratio of $\frac{2R_c}{2R_s + R_b + R_o}$ increases. Therefore, to obtain the same degree of accuracy the contacts must be as far apart as possible.

From these figures it is evident that the influence of sample thickness on the accuracy of the specific contact resistance is much less than the spacing of the contacts.

From these graphs a principal than does not only apply to CdTe but other materials as well is observed, namely that the increase in contact resistance as the contact area and contact separation decreases is clearly illustrated in figures 26, 27 and 28. Good ohmic contacts are essential in the manufacturing of very large scale integrated circuits (VLSI) since the contact resistance on that scale is much larger than the bulk or the spreading resistance.

The optimum mask design was not obtained since the mask used as illustrated in Fig. 22 yielded accuracy ranges for r_c that was sufficient on the material used to test the proposed method.

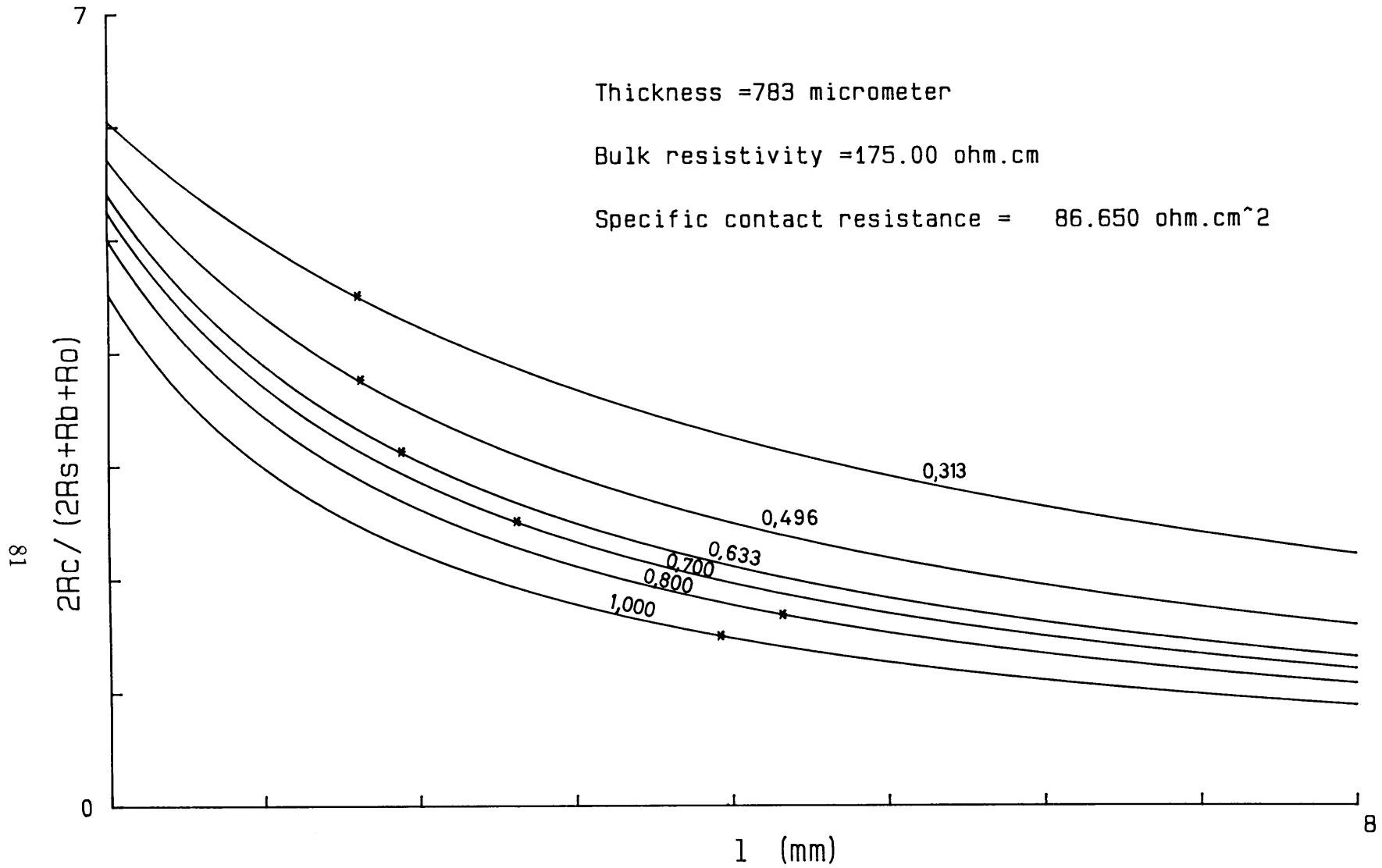


Fig 26 The graph of $\frac{2R_c}{2R_s + R_b + R_o}$ versus the contact separation l for six sets of contacts with 0.313 mm, 0.496 mm, 0.633 mm, 0.700 mm, 0.800 mm and 1.000 mm diameters. The stars indicate the ratio for each set of contacts for the mask as shown in Fig. 22 used on sample 6.1st

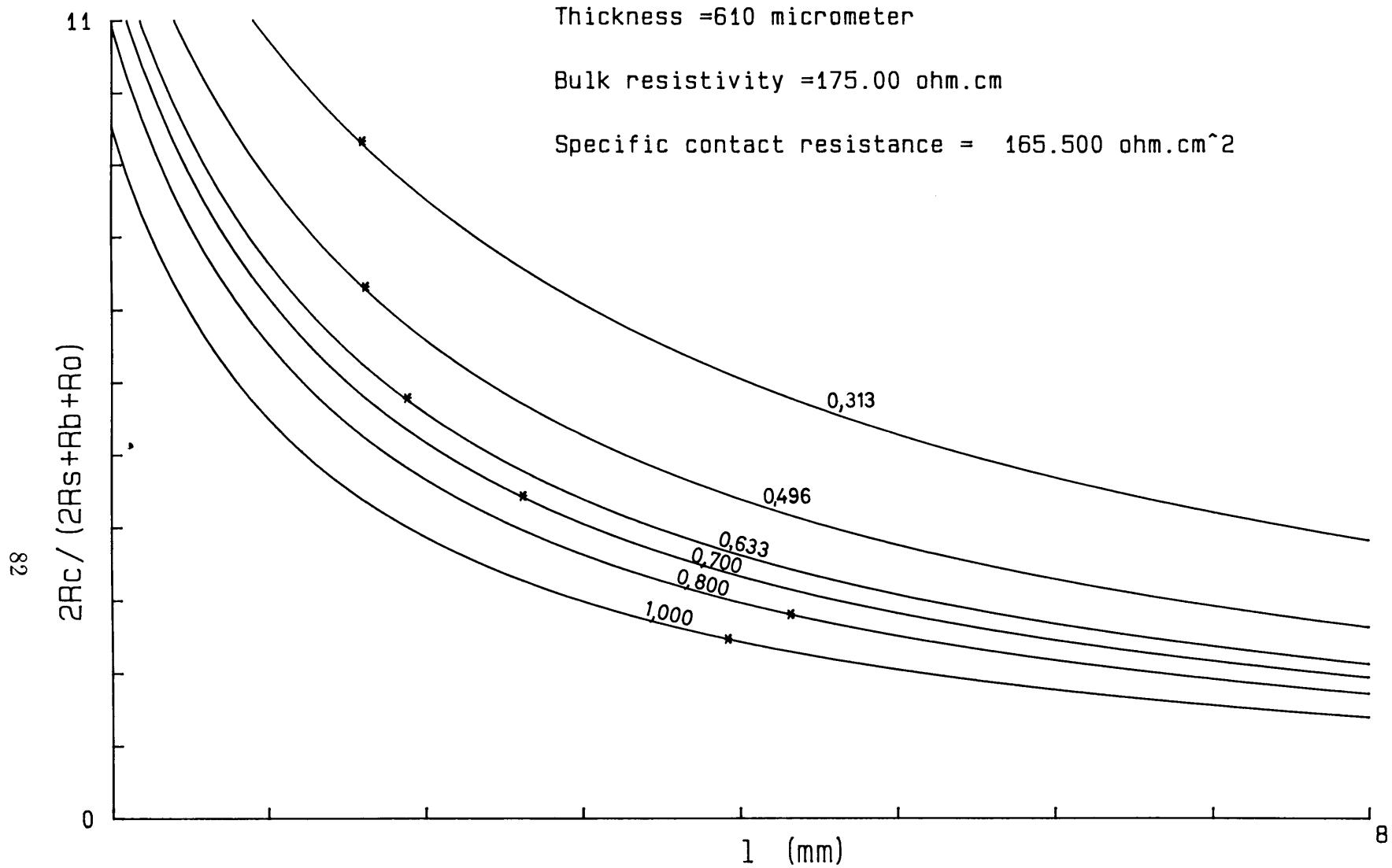


Fig 27 The graph of $\frac{2R_c}{2R_s + R_b + R_o}$ versus the contact separation l for six sets of contacts with 0.313 mm, 0.496 mm, 0.633 mm, 0.700 mm, 0.800 mm and 1.000 mm diameters. The stars indicate the ratio for each set of contacts for the mask as shown in Fig. 22 used on sample 6 2nd.

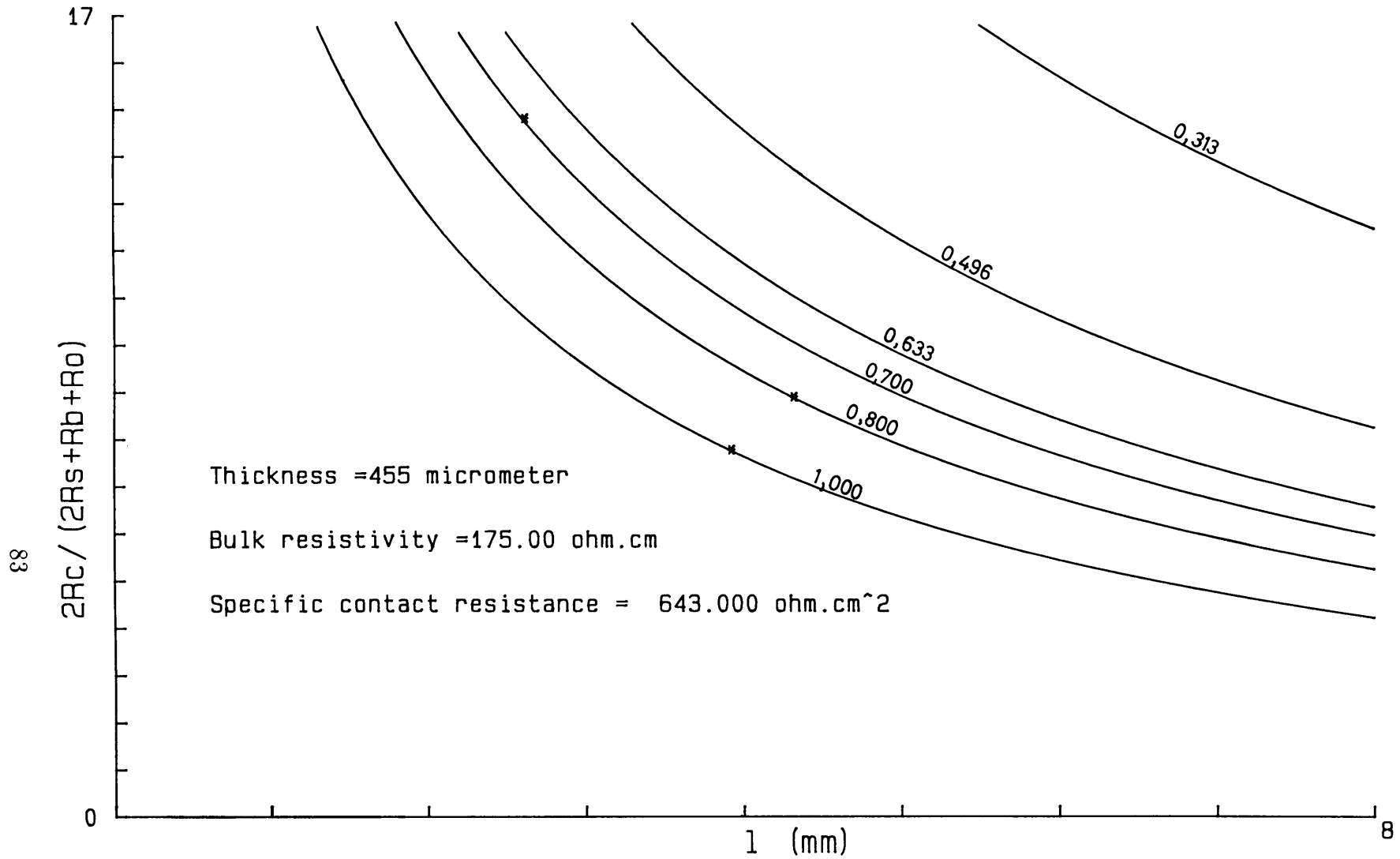


Fig 28 The graph of $\frac{2R_c}{2R_s + R_b + R_o}$ versus the contact separation l for six sets of contacts with 0.313 mm, 0.496 mm, 0.633 mm, 0.700 mm, 0.800 mm and 1.000 mm diameters. The stars indicate the ratio for each set of contacts for the mask as shown in Fig. 22 used on sample 6 3rd.

CHAPTER VII CONCLUSION

From this work it is clear that the manufacturing of good quality ohmic contacts onto CdTe and the determination of the specific contact resistance are by no means simple.

The sample preparation and contact manufacture procedures still need a fair amount of research. To assist with this it is necessary to use a reliable method to determine the specific contact resistance so that a good comparison between different preparation and manufacturing procedures can be made.

The methods discussed in chapter 2 have to be used with caution so as to obtain the most accurate result for the specific contact resistance r_c , since many of these methods make approximations that are not applicable or do not take the spreading resistance into account in their calculations. The simple method and the multi contact method do not include the spreading resistance in their calculations of r_c . Also the method of Jaeger and Seipp does not include the bulk resistance between the two contacts and makes an approximation to a planar current flow pattern which is only applicable to a radial current flow pattern. These above mentioned methods are therefore not recommended for the accurate and reliable calculation of r_c .

The method of Cox & Strack, Anthony et. al. and the transmission line method are recommended for the calculation of r_c for good ohmic contacts with values of r_c lower than 0.3ρ .

From the calculations in chapter 2 it is clear that the proposed method will be

a very appropriate method to use for contacts on CdTe if the numerical value of r_c is between 0.1ρ and 10.3ρ , where ρ is the bulk resistivity of the CdTe. The method was experimentally used in the range from 0.1ρ to 3.7ρ . The accuracy of these results will depend on the size of the contacts and the contact separation.

The quality of ohmic contacts is very much determined by the sample preparation procedure used. The quality of ohmic contacts manufactured on CdTe prepared by etching in dichromate is more or less ten times better than those on samples prepared with a Br:methanol etch.

When using a mechanical mask to manufacture two identical ohmic contacts the thickness of the mask must not be larger than $300\ \mu\text{m}$. When designing a mechanical mask to manufacture ohmic contacts, in order to obtain the same degree of accuracy, small diameter holes must be further apart than the larger diameter holes.

Comparing the current voltage characteristics of sample 1 and 3 it is observed that the Br:methanol etch results in an ohmic contact with a diode like behavior and the dichromate etch an ohmic like behavior.

ACKNOWLEDGEMENTS

I would like to thank the following institutions and individuals that assisted me with this work;

Department of Physics and E. M. Unit, University of the north, for the use of their facilities to perform most of the experimental work, the CdTe samples and the In, Cu and Au used.

The CSIR for the CdTe samples supplied and for the Hall– and Van der Pauw measurements performed by them.

Prof. Johan Malherbe from the department of Physics, Pretoria University , for performing the Auger electron spectroscopy.

REFERENCES

1. J. P. Ponpon, *Solid-State Electronics*, **28**, No. 7, 689–706 (1985)
2. A. L. Fahrenbruch, *Solar Cells*, **21**, 399–412 (1987)
3. G. Entine, P. Waar, T. Tierman and M. R. Squillante, *Nucl. Instrum. Methods Phys. Res. A, Accel. Spectrom. Detect. Assoc. Equip. A* **383**, No. 2, 282–290 (1989)
4. P. Siffert, *Mat. Res. Soc. Symp. Proc.*, **16**, 87–114 (1983)
5. N. C. Giles, S. Hwang, J. F. Schetzina, S. McDevitt and C. J. Johnson, *J. Appl. Phys.*, **64**, No. 5, 2656–2665 (1988)
6. R. H. Cox, H. Strack, *Solid-State Electron*, **21**, 715 (1978).
7. H. Jaeger and E. Seipp, *Journal of Electronic Materials*, **10**, No. 3, 606 (1981).
8. T. C. Anthony, A. L. Fahrenbruch and R. H. Bube, *Journal of Electronic Materials*, **11**, No. 1, 89 (1982)
9. L. K. Mak, C. M. Rogers and D. C. Northrop, *J. Phys. E: Sci. Instrum.*, **22**, 317–321 (1989)
10. H. Tews and C. An, *J. Appl. Phys.*, **53**, No. 7, 5339–5341 (1982)

11. B. L. Sharma, "Metal–Semiconductor Schottky Barrier Junctions and Their Applications".(Plenum Press,New York, 1984)
12. J. M. Andrews and J. C. Phillips, Chemical bonding and structure of metal– semiconductor interfaces, Phys. Rev. Lett., **35**, 56–59 (1975).
13. J. Bardeen, Phys. Rev., **71**, No. 10, 717–727 (1947).
14. S. Kurtin, T. C. McGill and C. A. Mead, Fundamental transition in electronic nature of solids, Phys. Rev. Lett., **22**, 1433–1436 (1969).
15. M. Aven and R. K. Swank, Proc. Electrochemical Society, **69** (1969)
16. R. Z. Bachrach, J. Vac. Sci. Technol., **15**, 1340 (1978).
17. J. van Laar, J. J. Scheer, Surf. Sci., **8**,342 (1976).
18. M. Henzler, Surf. Sci., **36**, 109 (1973).
19. R. Z. Bachrach, B. S. Krusor, J. Vac. Sci. Technol., **18**, 756 (1981).
20. C. B. Duke, Crit. Rev. Solid State Mater. Sci., **8**, 69 (1978).

21. D. J. Chadi, *J. Vac. Sci. Technol.*, **17**, 989 (1980).
22. D. E. Eastman, *J. Vac. Sci. Technol.*, **17**, (1979).
23. K. Mednick and L. Kleinman, *Phys. Rev.*, **B22**, 5768 (1980) : E.
B. Caruthers, L. Kleinman and G. P. Alldredge, *Phys. Rev.*, **B9**,
3330 (1974).
24. S. H. Wemple, *J. Electrochem. Soc.*, **115**, 241C (1968).
25. F. F. Morehead and G. Mandel, *Appl. Phys. Letters*, **5**, 53
(1964).
26. C. A. Mead, *Phys. Letters*, **6**, 103 (1965).
27. H. K. Henisch, "Semiconductor Contacts An Approach to Ideas
and Models", Clarendon Press, Oxford (1984)
28. P. M. Hall, *Thin Solid Films*, **1**, 277 (1967)
29. C. Y. Ting and C. Y. Chen, *Solid-State Electron.*, **14**, 433
(1971)
30. H. Kober, "Dictionary of Conformal Representations", Dover
Publishing Co., New York.(1957)

31. H. Murrmann and D. Widmann, *Solid–State Electron.*, **12**, 879 (1969)
32. H. H. Berger, *J. Electrochem. Soc.*, **119**, 507 (1972)
33. S. B. Schuldt, *Solid–State Electron.*, **21**, 715 (1978)
34. Y. K. Fang, C. Y. Chang, and Y. K. Su, *Solid–State Electron.*, **22**, 933 (1979)
35. H. C. Montgomery, *Solid–State Electronics*, **7**, 147–152 (1964)
36. S. Nazaki, A. G. Milnes, *Journal of Electronic Materials*, **14**, No. 2, 137–155 (19)
37. M. Tomitori, M. Kuriki and S. Hayakawa, *Japanese Journal of Applied Physics*, **26**, No. 4, 588–591 (1987)
38. R. E. Braithwaite, C. G. Scott and J. B. Mullin, *Solid–State Electronics*, **23**, 1091–1092 (1980)
39. D. de Nobel, *Philips Res. Repts.*, **14**, 361 (1959)
40. N. M. Forsyth, I. M. Dharmadasa, Z. Sobiesierski and R. H. Williams, *Vacuum*, **38**, No. 4/5, 369–371 (1988)
41. A. M. Mancini et. al., *J. Appl. Phys.*, **53**, No. 8, 5785 (1982)

42. A. Musa, J. P. Ponpon, J. J. Grob, M. Hage—Ali, R. Stuck and P. Siffert, *J. Appl. Phys.*, **54**, No. 6, 3260—3268 (1983)
43. J. Gu, T. Kitahara, K. Kawakami and T. Sakaguchi, *Journal of Applied Physics*, **46**, No. 3, 1184—1185 (1975)
44. R. H. Williams, I. M. Dharmadasa, M. H. Patterson, C. Maani and N. M. Forsyth, *Surface Science*, **168**, 323—335 (1986)
45. J. P. Ponpon, M. Saraphy, E. Buttung and P. Siffert, *Phys. Stat. Sol. (a)*, **59**, 259 (1980)
46. T. L. Chu and S. S. Chu, *J. Appl. Phys.*, **58**, No. 11, 4296 (1985)
47. B. M. Basol, S. S. Ou and O. M. Stafsudd, *J. Appl. Phys.*, **58**, No. 10, 3809 (1985)
48. M. Hansen, "Constitution of Binary Alloys", McGraw—Hill (1958)
49. D. Brigs and M. P. Seah, "Practical surface analysis", John Wiley 1985.
50. T. Moeller, "Inorganic Chemistry", Wiley, Fourth Printing,(1955)
51. M. E. Lee, To be published.